Annual Report

Low Temperature Deposition and Characterization of N- and P-Type Silicon Carbide Thin Films and Associated Ohmic and Schottky Contacts

Supported under Grant #N00014-92-J-1500
Office of the Chief of Naval Research
Report for the period January 1, 1992–December 31, 1992

R. F. Davis and R. J. Nemanich*
R. S. Kern, R. Patterson, L. B. Rowland,
L. Spellman-Porter, and S. Tanaka
Materials Science and Engineering Department
*Department of Physics
North Carolina State University
Raleigh, NC 27695

December, 1992

REPORT DOCUMENTATION PAGE

Form Approved
OMB No 0704 0188

1. AGENCY USE ONLY (Leave blank)	2. REPORT DATE	3. REPORT TYPE AND DATES COVERED
	January, 1992	Annual—January 1, 1992–December 31, 1992

4. TITLE AND SUBTITLE
Low Temperature Deposition and Characterization of N- and P-Type Silicon Carbide Thin Films and Associated Ohmic and Schottky Contacts

5. FUNDING NUMBERS
R&T: sic0002---01
1261
N00179
N66005
4B855

6. AUTHOR(S)
Robert F. Davis

7. PERFORMING ORGANIZATION NAME(S) AND ADDRESS(ES)
North Carolina State University
Hillsborough Street
Raleigh, NC 27695

8. PERFORMING ORGANIZATION REPORT NUMBER
#N00014-92-J-1500

9. SPONSORING/MONITORING AGENCY NAME(S) AND ADDRESS(ES)
Sponsoring: ONR, 800 N. Quincy, Arlington, VA 22217
Monitoring: Office of Naval Research Resider, N66005
The Ohio State Univ. Research Center
1314 Kinnear Road
Columbus, OH 43212-1194

10. SPONSORING/MONITORING AGENCY REPORT NUMBER

11. SUPPLEMENTARY NOTES

12a. DISTRIBUTION/AVAILABILITY STATEMENT
Approved for Public Release—Distribution Unlimited

12b. DISTRIBUTION CODE

13. ABSTRACT *(Maximum 200 words)*

Single-crystal epitaxial films of cubic β(3C)-SiC(111) and AlN(0001) have been deposited on α(6H)-SiC(0001) substrates oriented 3-4° towards [11$\bar{2}$0] at 1050°C via gas-source molecular beam epitaxy using disilane (Si_2H_6), ethylene (C_2H_4), thermal evaporation of Al and activated N species derived from an ECR plasma. High resolution transmission electron microscopy revealed that the nucleation and growth of the β(3C)-SiC regions occurred primarily on terraces between closely spaced steps. Pseudomorphic bilayer structures containing β(3C)-SiC and 2H-AlN have been grown under the same conditions for the first time. HREED and cross-sectional HRTEM showed all layers to be monocrystalline. Initial high temperature chemical interdiffusion studies between SiC and AlN show that all components diffuse very slowly across the interface. AHRTEM and SAS are being used to determine the concentration profiles. Thin film solid solutions of AlN and SiC have been deposited using similar techniques and conditions as the individual compounds. Metal contacts of Ti, Pt and Hf deposited at RT on n-type α(6H)-SiC(0001) exhibit rectifying behavior with ideality factors between 1.01 and 1.09. The Pt and Hf contacts had leakage currents of 5×10^{-8} A/cm^2 at -10V. Values of barrier heights for all contacts were within a few tenths of 1.0eV which is indicative that the Fermi level is pinned at the SiC surface.

14. SUBJECT TERMS	15. NUMBER OF PAGES
films, SiC, AlN, gas source molecular beam epitaxy, transmission electron microscopy, chemical interdiffusion, metal contacts, Ti, Pt, Hf, ideality factors, Fermi level pinning	62
	16. PRICE CODE

17. SECURITY CLASSIFICATION OF REPORT	18. SECURITY CLASSIFICATION OF THIS PAGE	19. SECURITY CLASSIFICATION OF ABSTRACT	20. LIMITATION OF ABSTRACT
UNCLAS	UNCLAS	UNCLAS	SAR

Table of Contents

I. Introduction

Silicon carbide (SiC) is a wide bandgap material that exhibits polytypism, a one-dimensional polymorphism arising from the various possible stacking sequences of the silicon and carbon layers. The lone cubic polytype, β-SiC, crystallizes in the zincblende structure and is commonly referred to as 3C-SiC. In addition, there are also approximately 250 other rhombohedral and hexagonal polytypes [1] that are all classed under the heading of α-SiC. The most common of the α-SiC polytypes is 6H-SiC, where the 6 refers to the number of Si/C bilayers along the closest packed direction in the unit cell and the H indicates that the crystal structure is hexagonal.

Beta (3C)-SiC is of considerable interest for electronic applications that utilize its attractive physical and electronic properties such as wide bandgap (2.2 eV at 300K) [2], high breakdown electric field (2.5×10^6 V/cm) [3], high thermal conductivity (3.9 W/cm °C) [4], high melting point (3103K at 30 atm) [5], high saturated drift velocity (2×10^7 m/s) [6], and small dielectric constant (9.7) [7]. Primarily due to its higher electron mobility than that of the hexagonal polytypes, such as 6H-SiC [8], β-SiC remains preferable to hexagonal SiC for most device applications.

Most 3C-SiC thin film growth to date has been performed on Si substrates. Large-area, crack-free, and relatively thick (up to 30 μm) epitaxial 3C-SiC thin films have been grown on Si (100) by exposing the Si substrate to a C-bearing gaseous species prior to further SiC growth [7, 9, 10]. However, these films exhibited large numbers of line and planar defects due to large lattice and thermal mismatches between SiC and Si. One particular type of planar defect, the inversion domain boundary (IDB), was eliminated with the use of Si (100) substrates cut 2°–4° toward [011] [11-13]. Growth on Si substrates has allowed much understanding of SiC growth processes and device development to occur, but the large thermal and lattice mismatches between SiC and Si hamper further development using Si substrates. As a result, great effort has been made to develop methods for growth SiC single crystal substrates for homoepitaxial growth of SiC thin films.

Since the 1950's, monocrystalline single crystals of 6H-SiC have been grown at using the Lely sublimation process [14]. However, nucleation was uncontrolled using this process and control of resultant polytypes was difficult. SiC single crystals inadvertently formed during the industrial Acheson process have also been used as substrates for SiC growth. However, neither these crystals or those formed using the Lely process are large enough for practical device applications. Recently, using a seeded sublimation-growth process, boules of single polytype 6H-SiC of > 1 inch diameter of much higher quality of that obtained using the Lely process have been grown. The use of single crystals of the 6H polytype cut from these boules has given a significant boost to SiC device development.

SiC epitaxial thin film growth on hexagonal SiC substrates has been reported since the

1960's. The use of nominally on-axis SiC substrates has usually resulted in growth of 3C-SiC films. Films of 3C-SiC (111) grown by CVD have been formed on 6H-SiC substrates less than 1° off (0001) [15]. Films of 3C-SiC on 6H-SiC substrates have typically had much lower defect densities than those grown on Si substrates. The major defects present in 3C-SiC/6H-SiC films have been double positioning boundaries (DPB) [16]. Despite the presence of DPBs, the resultant material was of sufficient quality to further device development of SiC. The use of off-axis 6H-SiC (0001) substrates has resulted in growth of high-quality monocrystalline 6H-SiC layers with very low defect densities [17].

In addition, the use of more advanced deposition techniques, such as molecular beam epitaxy (MBE), has been reported for SiC in order to reduce the growth temperature and from about 1400-1500°C on 6H-SiC substrates. Si and C electron-beam sources have been used to epitaxially deposit SiC on 6H-SiC (0001) at temperatures of 1150°C [18]. Ion-beam deposition of epitaxial 3C-SiC on 6H-SiC has also been obtained at the temperature of 750°C using mass-separated ion beams of $^{30}Si^{+}$ and $^{13}C^{+}$ [19].

Aluminum nitride (AlN) is also of particular interest at this time because of its very large bandgap. It is the only intermediate phase in the Al-N system and normally forms in the wurtzite (2H-AlN) structure. Most current uses of AlN center on its mechanical properties, such as high hardness (9 on Mohs scale), chemical stability, and decomposition temperature of about 2000°C [20]. Properties such as high electrical resistivity (typically $\geq 10^{13}$ Ω-cm), high thermal conductivity (3.2 W/cm K) [21], and low dielectric constant ($\varepsilon \approx 9.0$) make it useful as a potential substrate material for semiconductor devices as well as for heat sinks. The wurtzite form has a bandgap of 6.28 eV [22] and is a direct transition, thus it is of great interest for optoelectronic applications in the ultraviolet region.

Because of the difference in bandgaps (2.28 eV for 3C-SiC and 6.28 eV for 2H-AlN) between the materials, a considerable range of wide bandgap materials, made with these materials, should be possible. Two procedures for bandgap engineering are solid solutions and multilayers. A particularly important factor is that the two materials have a lattice mismatch of less than one percent.

Research in ceramic systems suggests that complete solid solubility of AlN in SiC may exist [23]. Solid solutions of the wurtzite crystal structure should have E_g from 3.33 eV to 6.28 eV at 0 K. Although it has not been measured, the bandgap of cubic AlN has been estimated to be around 5.11 eV at absolute zero and is believed to be indirect [24]. Cubic solid solutions should thus have E_g from 2.28 eV to roughly 5.11 eV at 0 K and would be indirect at all compositions if theory holds true.

Because of their similarity in structure and close lattice and thermal match, AlN-SiC heterostructures are feasible for electronic and optoelectronic devices in the blue and infrared region. Monocrystalline AlN layers have been formed by CVD on SiC substrates [25] and SiC

layers have been formed on AlN substrates formed by AlN sputtering on single crystal W [26]. In addition, theory on electronic structure and bonding at SiC/AlN interfaces [24] exists and critical layer thicknesses for misfit dislocation formation have been calculated for cubic AlN/SiC [27]. Note that AlN (at least in the wurtzite structure) is a direct-gap material and SiC is an indirect gap material. Superlattices of these materials would have a different band structure than either constituent element. The Brillouin zone of a superlattice in the direction normal to the interfaces is reduced in size. This reduction in zone size relative to bulk semiconductors causes the superlattice bands to be "folded into" this new, smaller zone. This folding can cause certain superlattice states to occur at different points in k space than the corresponding bulk material states [28]. This can lead to direct transitions between materials which in the bulk form have indirect transitions. This has been demonstrated in the case of $GaAs_{0.4}P_{0.6}$/GaP and $GaAs_{0.2}P_{0.8}$/GaP superlattices, where both constituents are indirect in the bulk form [29]. Whether this is possible in the case of AlN/SiC is unknown, but very intriguing. It may be possible to obtain direct transitions throughout nearly the entire bandgap range with use of superlattices of AlN and SiC. Use of solid solutions in superlattices introduces additional degrees of freedom. For example, the bandgap can be varied independently of the lattice constant with proper choice of layer thickness and composition if superlattices of solid solutions of AlN and SiC were formed.

Due to the potential applications of solid solutions and superlattice structures of these two materials, an MBE/ALE system was commissioned, designed, and constructed for growth of the individual compounds of SiC and AlN, as well as solid solutions and heterostructures of these two materials. Dithisimal studies concerned with the kinetics and mechanisms of mass transport of Si, C, Al and N at the SiC/AlN interface are also being conducted in tandem with the deposition investigations.

A very important additional goal of this research is to understand what controls the contact electrical characteristics of specific metals to n-type 6H-SiC and to use this information to form good ohmic and Schottky contacts. A list of five metals to be studied, which consists of Ti, Pt, Hf, Co, and Sr, was created at the beginning of this research project. The selection process began by taking the simplest case, an ideal contact which behaves according to Schottky-Mott theory. This theory proposes that when an intimate metal-semiconductor contact is made the Fermi levels align, creating an energy barrier equal to the difference between the workfunction of the metal and the electron affinity of the semiconductor. It is the height of this barrier which determines how the contact will behave; for ohmic contacts it is desirable to have either no barrier or a negative barrier to electron flow, while for a good Schottky contact a large barrier is desired.

Although metals were chosen optimistically, i.e. on the basis that they will form ideal contacts, some evidence exists that the contact properties will be more complicated. J. Pelletier

et al. [30] have reported Fermi level pinning in 6H-SiC due to intrinsic surface states, suggesting little dependence of barrier height on the workfunction of the metal. In addition, L. J. Brillson [31, 32] predicts the pinning rate to be higher for more covalently bonded materials. Other complications may arise if the surface is not chemically pristine. A major part of this project will be devoted to determining whether the contacts behave at all ideally, and if not, whether the Fermi level is pinned by intrinsic or extrinsic effects.

Along with examining the barriers of the pure metal contacts, the chemistry upon annealing will be studied and correlated with the resulting electrical behavior. The electrical behavior will be quantified both macroscopically in terms of current-voltage characteristics and microscopically in terms of barrier height. Identification of the phases formed will present the opportunity to attribute the electrical characteristics to the new phase in contact with silicon carbide.

Within this reporting period, 3C-SiC and AlN thin films were grown on single crystal wafers of 6H-SiC cut 3°-4° off (0001) towards [11$\bar{2}$0]. The crystalline quality of these films as determined using reflection high-energy electron diffraction (RHEED). Surface morphology was examined using scanning electron microscopy (SEM). Defects and interfaces were characterized using high-resolution transmission electron microscopy (HRTEM). From this analysis, reasons are discussed for the formation of 3C-SiC despite the presence of large numbers of surface steps on off-axis substrates. Research concerned with the growth of $(AlN)_x(SiC)_{1-x}$ solid solutions and AlN/SiC heterostructures has also been conducted as well as chemical interdiffusion between these phases. Lastly, the results of the investigations concerned with the use of Ti, Pt and Hf metals as rectifying contacts on n-type 6H-SiC are described. Several techniques have been and are being implemented to measure barrier heights. Electrical measurements will be presented, along with some observed trends. The experimental procedures, results, discussion of these results, conclusions and plans for future efforts for each of the topics noted above are presented in the following sections. Each of these sections is self-contained with its own figures, tables and references.

REFERENCES

1. G. R. Fisher and P. Barnes, Philos. Mag. B **61**, 217 (1990).
2. H. P. Philipp and E. A. Taft, in *Silicon Carbide, A High Temperature Semiconductor*, edited by J. R. O'Connor and J. Smiltens (Pergamon, New York, 1960), p. 371.
3. W. von Muench and I. Pfaffender, J. Appl. Phys. **48**, 4831 (1977).
4. E. A. Bergemeister, W. von Muench, and E. Pettenpaul, J. Appl. Phys. **50**, 5790 (1974).
5. R. I. Skace and G. A. Slack, in *Silicon Carbide, A High Temperature Semiconductor*, edited by J. R. O'Connor and J. Smiltens (Pergamon, New York, 1960), p. 24.
6. W. von Muench and E. Pettenpaul, J. Appl. Phys. **48**, 4823 (1977).
7. S. Nishino, Y. Hazuki, H. Matsunami, and T. Tanaka, J. Electrochem Soc. **127**, 2674 (1980).

8. P. Das and K. Ferry, Solid State Electronics, **19**, 851 (1976).
9. K. Sasaki, E. Sakuma, S. Misawa, S. Yoshida, and S. Gonda, Appl. Phys. Lett. **45**, 72 (1984).
10. P. Liaw and R. F. Davis, J. Electrochem. Soc. **132**, 642 (1985).
11. K. Shibahara, S. Nishino, and H. Matsunami, J. Cryst. Growth **78**, 538 (1986).
12. J. A. Powell, L. G. Matus, M. A. Kuczmarski, C. M. Chorey, T. T. Cheng, and P. Pirouz, Appl. Phys. Lett. 51, 823 (1987).
13. H. S. Kong, Y. C. Wang, J. T. Glass, and R. F. Davis, J. Mater. Res **3**, 521 (1988).
14. J. A. Lely, Ber. Deut. Keram. Ges. **32**, 229 (1955).
15. H. S. Kong, J. T. Glass, and R. F. Davis, Appl. Phys. Lett. **49**, 1074 (1986).
16. H. S. Kong, B. L. Jiang, J. T. Glass, G. A. Rozgonyi, and K. L. More, J. Appl. Phys. **63**, 2645 (1988).
17. H. S. Kong, J. T. Glass, and R. F. Davis, J. Appl. Phys. **64**, 2672 (1988).
18. S. Kaneda, Y. Sakamoto, T. Mihara, and T. Tanaka, J. Cryst. Growth **81**, 536 (1987).
19. S. P. Withrow, K. L. More, R. A. Zuhr, and T. E. Haynes, Vacuum **39**, 1065 (1990).
20. C. F. Cline and J. S. Kahn, J. Electrochem. Soc, **110**, 773 (1963).
21. G. A. Slack, J. Phys. Chem. Solids **34**, 321 (1973).
22. W. M. Yim, E. J. Stofko, P. J. Zanzucci, J. I. Pankove, M. Ettenberg, and S. L. Gilbert, J. Appl. Phys. **44**, 292 (1973).
23. See, for example, R. Ruh and A. Zangvil, J. Am. Ceram. Soc. **65**, 260 (1982).
24. W. R. L. Lambrecht and B. Segall, Phys. Rev. B **43**, 7070 (1991).
25. T. L. Chu, D. W. Ing, and A. J. Norieka, Solid-State Electron. **10**, 1023 (1967).
26. R. F. Rutz and J. J. Cuomo, in *Silicon Carbide-1973*, ed. by R. C. Marshall, J. W. Faust, Jr., and C. E. Ryan, Univ. of South Carolina Press, Columbia, p. 72 (1974).
27. M. E. Sherwin and T. J. Drummond, J. Appl. Phys. **69**, 8423 (1991).
28. G. C. Osbourn, J. Vac. Sci. Technol. B **1**, 379 (1983).
29. P. L. Gourley, R. M. Biefeld, G. C. Osbourn, and I. J. Fritz, *Proceedings of 1982 Int'l Symposium on GaAs and Related Compounds* (Institute of Physics, Berkshire, 1983), p. 248.
30. J. Pelletier, D. Gervais, and C. Pomot, J. Appl. **55**, 994 (1984).
31. L. J. Brillson, Phys. Rev. B, **18**, 2431 (1978).
32. L. J. Brillson, Surf. Sci. Rep., **2**, 123 (1982).

II. Gas-Source Molecular Beam Epitaxy of Monocrystalline Beta-SiC on Vicinal Alpha(6H)-SiC

A Communication
Submitted for Consideration for Publication
to
The Journal of Materials Research

By

L. B. Rowland*, S. Tanaka, R. S. Kern and Robert F. Davis
Department of Materials Science and Engineering
North Carolina State University
Box 7907
Raleigh, North Carolina 27695-7907

November, 1992

ABSTRACT

Single-crystal epitaxial films of cubic β(3C)-SiC(111) have been deposited on hexagonal α(6H)-SiC(0001) substrates oriented 3-4° towards [11$\bar{2}$0] at 1050-1250°C via gas-source molecular beam epitaxy using disilane (Si_2H_6) and ethylene (C_2H_4). High resolution transmission electron microscopy revealed that the nucleation and growth of the β(3C)-SiC regions occurred primarily on terraces between closely spaced steps because of reduced rates of surface migration at the low growth temperatures. Double positioning boundaries were observed at the intersections of these regions.

*Present Address
Naval Research Laboratory, Code 6861
4555 Overlook Av., SW
Washington, DC 20375-5320

Polytypes are special one-dimensional polymorphs which differ only in the stacking sequence along the closest-packed direction. Silicon carbide occurs in one cubic (zincblende) polytype referred to as 3C- or β-SiC, where the 3 refers to the number of planes in the periodic sequence. The hexagonal (wurtzite) polytype also exists in this material. Both polytypes occur in more complex, intermixed forms yielding a wider range of ordered, larger period, hexagonal or rhombohedral structures of which 6H is the most common. All of these noncubic polytypes are known collectively as α-SiC.

The growth of 3C- and 6H-SiC thin films has been achieved primarily via chemical vapor deposition (CVD) (see Ref. #1 for a review of this research). Monocrystalline Si(100) wafers have been the principal substrate of choice for the deposition of 3C. It is now a common first step to transform the surface region of these wafers to β-SiC by reaction with a C-containing gas to reduce the effects of the large mismatches in lattice parameters (≈20%) and coefficients of thermal expansion (≈10%). The epitaxial growth of SiC films on α(6H)-SiC(0001) substrates via CVD has been reported for three decades[1]. Single phase β-SiC films result[2,3] when the [0001] direction of the 6H wafer is oriented off-axis ≤1°. The primary defects in these films are double positioning boundaries (DPB)[4]. The use of vicinal 6H-SiC(0001) substrates cut 3-4° towards [11$\bar{2}$0] have resulted in high-quality monocrystalline 6H-SiC layers with low defect densities[5,6], including the absence of DPBs.

Solid- and gas-source (GS) molecular beam epitaxy (MBE) techniques have also been employed for deposition of SiC films[7,8]. Kaneda et al.[7] used on-axis α(6H)-SiC{0001} substrates and electron-beam evaporated Si and C sources. Epitaxial 3C-SiC(111) films were obtained at particular Si-to-C flux ratios in the temperature range of 1150-1400°C, as determined by reflection high-energy electron diffraction (RHEED). No information was given by these authors regarding either the microstructure or the type of defects present in these films. By contrast, Yoshinobu et al.[8] employed the periodic introduction of Si_2H_6 and C_2H_2 to achieve 3C-SiC growth on vicinal 6H-SiC(000$\bar{1}$) and 6H-SiC(0$\bar{1}$14) substrates at 850-1160°C. Films grown on vicinal 6H-SiC (000$\bar{1}$) contained DPBs while those grown on 6H-SiC (0$\bar{1}$14) were free of these defects. Smooth films were obtained at the lowest growth rates used in the study (< 0.01 μm/hr).

In the present research, the 3C-SiC films were grown via GSMBE between 1050 and 1250°C on α(6H)-SiC(0001) wafers oriented 3-4° off [0001] towards [11$\bar{2}$0] and produced by Cree Research, Inc.using a seeded Lely sublimation method. The MBE growth system has been described previously[9]. Each wafer was sequentially cleaned prior to growth using a 10% HF etch at room temperature for 5 min, rinsed in DI water for 2 min and heated in the MBE chamber for 5 min at the growth temperature to achieve the desorption and decomposition of any remaining hydrocarbon species and native oxide, respectively. The source gases of Si_2H_6

and C_2H_4 were used to deposit the SiC. The base and operating pressures were 10^{-9} torr and 3×10^{-5}-3×10^{-6} torr, respectively.

The surface morphology was determined using field-emission scanning electron microscopy (SEM) at an operating voltage of 2.0 kV. Reflection high-energy electron diffraction (RHEED) at 10 kV and high-resolution transmission electron microscopy (HRTEM) were used for structure and microstructure analyses. Samples were prepared for HRTEM using standard techniques[10]. An Akashi EM 002B high-resolution transmission electron microscope was used at 200 kV for the HRTEM analysis.

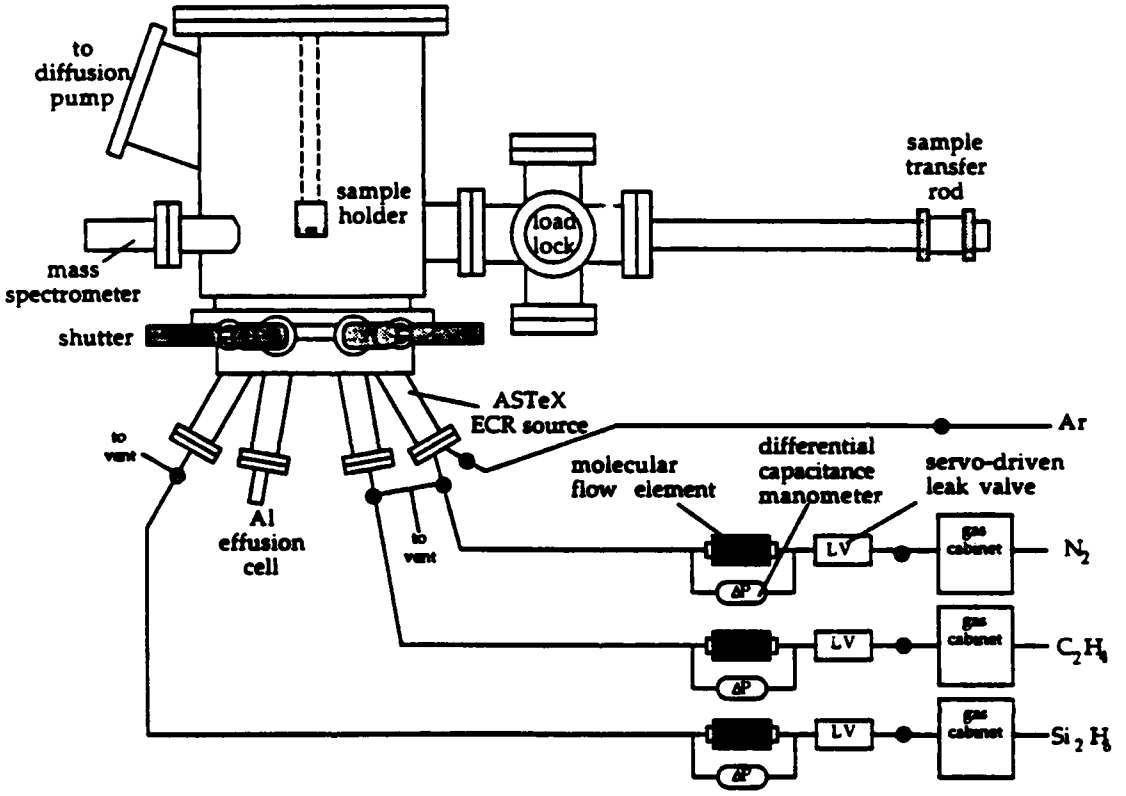

Figure 1. Schematic of molecular beam epitaxy system.

The films grown in this study were single crystal SiC as determined by HRTEM and/or RHEED. The surfaces of all films appeared smooth and specular to the naked eye. The surface morphologies of samples grown at 1250°C using the Si:C flow rate ratio of 1:2 are shown in Figure 2. The use of a total flow rate of 3.0 sccm resulted in a rough surface containing a high density of small (0.1-0.2 μm) triangular regions of different heights, as shown in Figure 2(a). Reducing the total flow rate to 1.5 sccm produced a smoother top surface with regions of uniform height, as shown in Fig. 2(b). Further reduction to 0.30 sccm resulted in a significantly smoother surface with fewer, smaller regions (Figure 2(c)). The use of 0.06 sccm did not result in growth, as determined by HRTEM analysis.

(a)

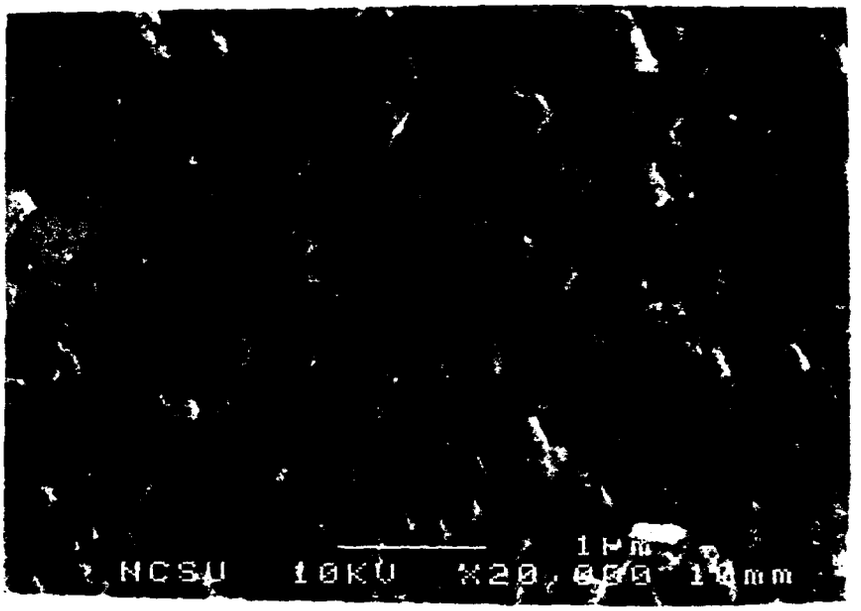

(b)

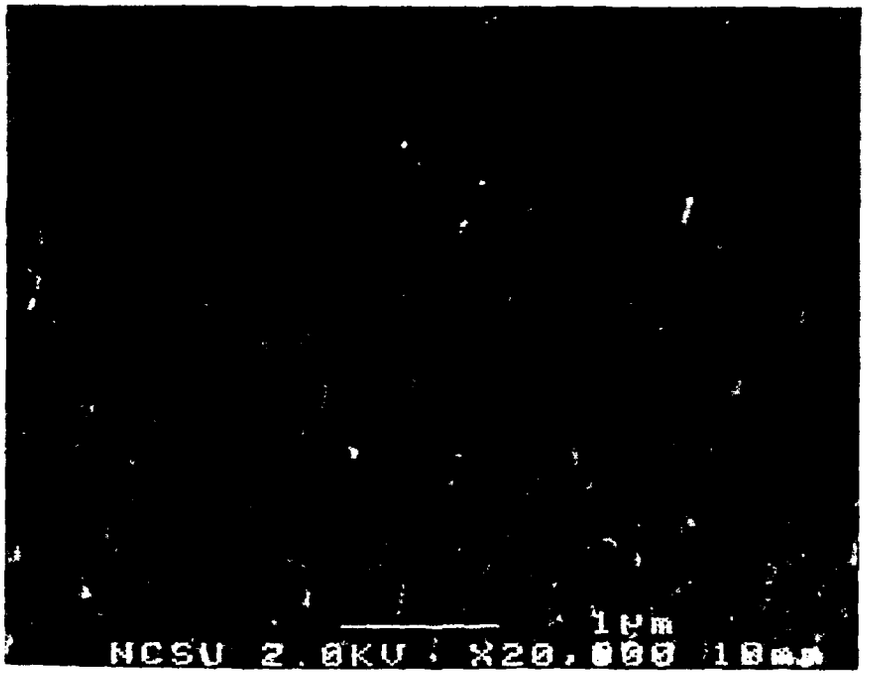

Figure 2. Scanning electron micrograph of the surface of 3C-SiC films grown on 3-4° off-axis 6H-SiC substrates at 1250°C using (a) 2.0 sccm C_2H_4 and 1.0 sccm Si_2H_6, (b) 1.0 sccm C_2H_4 and 0.5 sccm Si_2H_6.

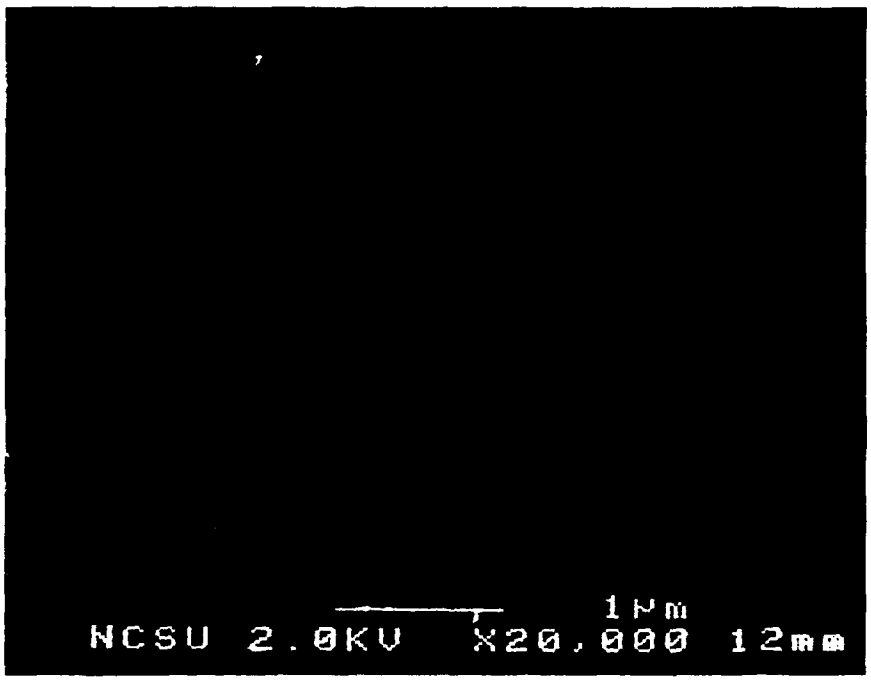

Figure 2(c). 0.2 sccm C_2H_4 and 0.1 sccm Si_2H_6.

Figure 3 is a cross-sectional HRTEM micrograph of the SiC film grown at 1250°C using a total flow rate of 1.5 sccm. The substrate is oriented so that the [11$\bar{2}$0] direction is perpendicular to the plane of the image. The lattice images of the film reveal it to be the β(3C) polytype in the (111) orientation. The micrograph and the corresponding selected-area diffraction pattern also show the epitaxial relationship between the substrate and the film. Stacking faults parallel to the interface can also be observed. Plan-view TEM on this sample (Figure 4) shown that DPBs and stacking faults (denoted SF) are present in this sample. The same results were obtained at all growth temperatures using the C:Si flow rate ratio of 2:1.

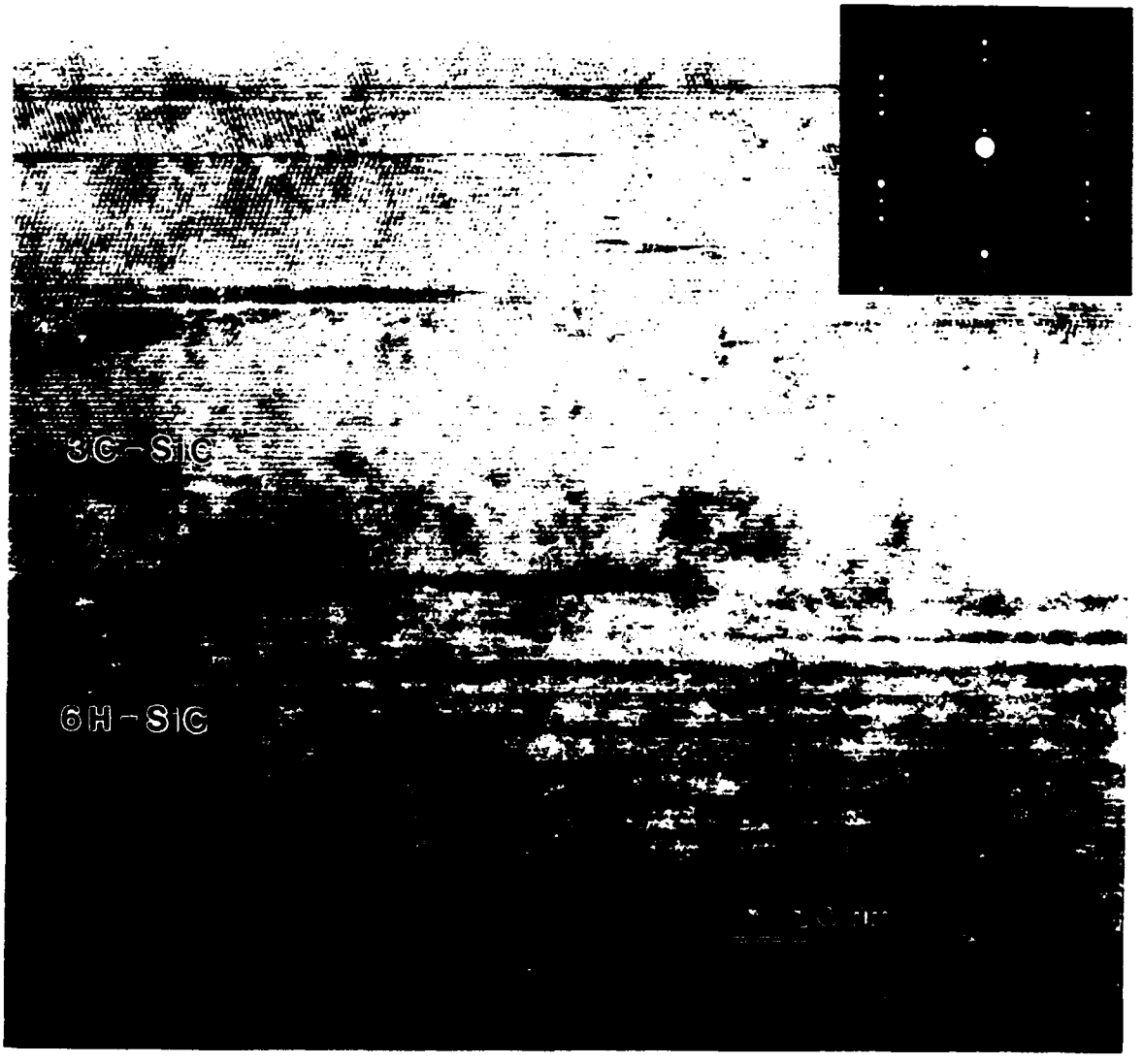

Figure 3. Cross-sectional HRTEM micrograph of 3C-SiC (111) film on vicinal 6H-SiC (0001) substrate with inset of selected area diffraction pattern ([110] zone axis). Sample was grown at 1250°C using 1.0 sccm C_2H_4 and 0.5 sccm Si_2H_6.

Figure 4. Plan-view transmission electron micrograph of 3C-SiC film and 6H-SiC substrate shown in Figure 3. Both stacking faults (denoted SF) and double positioning boundaries (denoted DPB) are visible.

The occurrence of 3C-SiC on vicinal α(6H)-SiC substrates is in contrast to the 6H films obtained by CVD, where step separation clearly defines the stacking sequence of the resulting films[5,6]. It was initially believed that a decrease in total flow rate at the same growth temperature would allow the 6H polytype to form, as the Si and C species would have more time to reach energetically favorable sites associated with steps. However, the 3C polytype formed regardless of the total flow rate. Growth at 1200 and 1050°C under similar conditions also resulted in 3C-SiC.

Films were also grown at 1050°C using the flow rates of 2.0 sccm C_2H_4 and 0.50 sccm Si_2H_6. The decrease in temperature and the high flow rate were used to lower the reactivity and surface mobility and to increase the supply of precursor species, respectively, to enhance the nucleation density. An SEM micrograph of the surface of this film is shown in Figure 5. The film appears much smoother than films grown at higher temperature and/or at lower flow rates. However, individual regions are also observed with diameters of substantially less than 100 nm. The HRTEM microstructure of this film shown in Figure 6 reveals a high density of steps (denoted by arrows) on the substrate surface and regions of 3C-SiC(111) which are entered on the terraces between the steps. Each terrace appears to have one individual region. In most

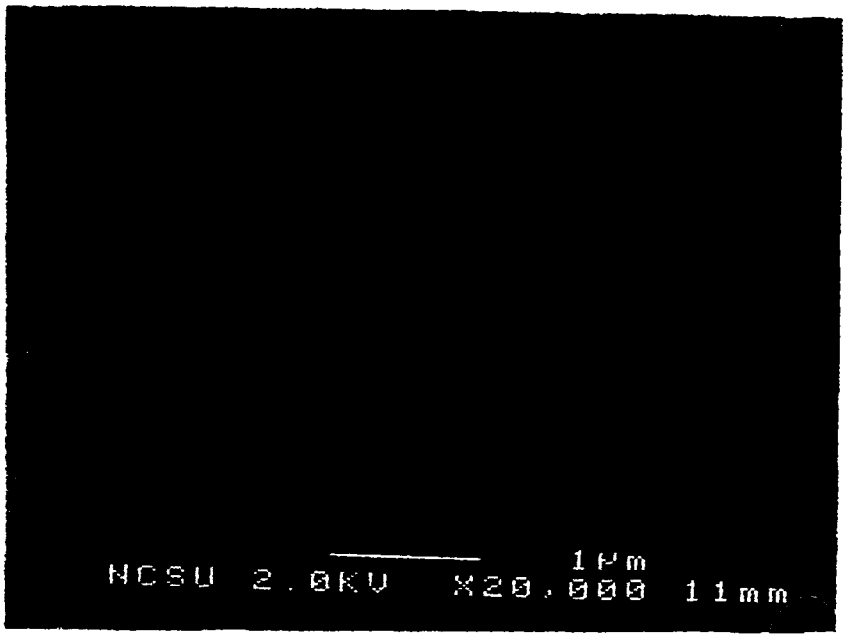

Figure 5. Scanning electron micrograph of surface of 3C-SiC film grown on vicinal 6H-SiC at 1050°C using 2.0 sccm C_2H_4 and 0.5 sccm Si_2H_6.

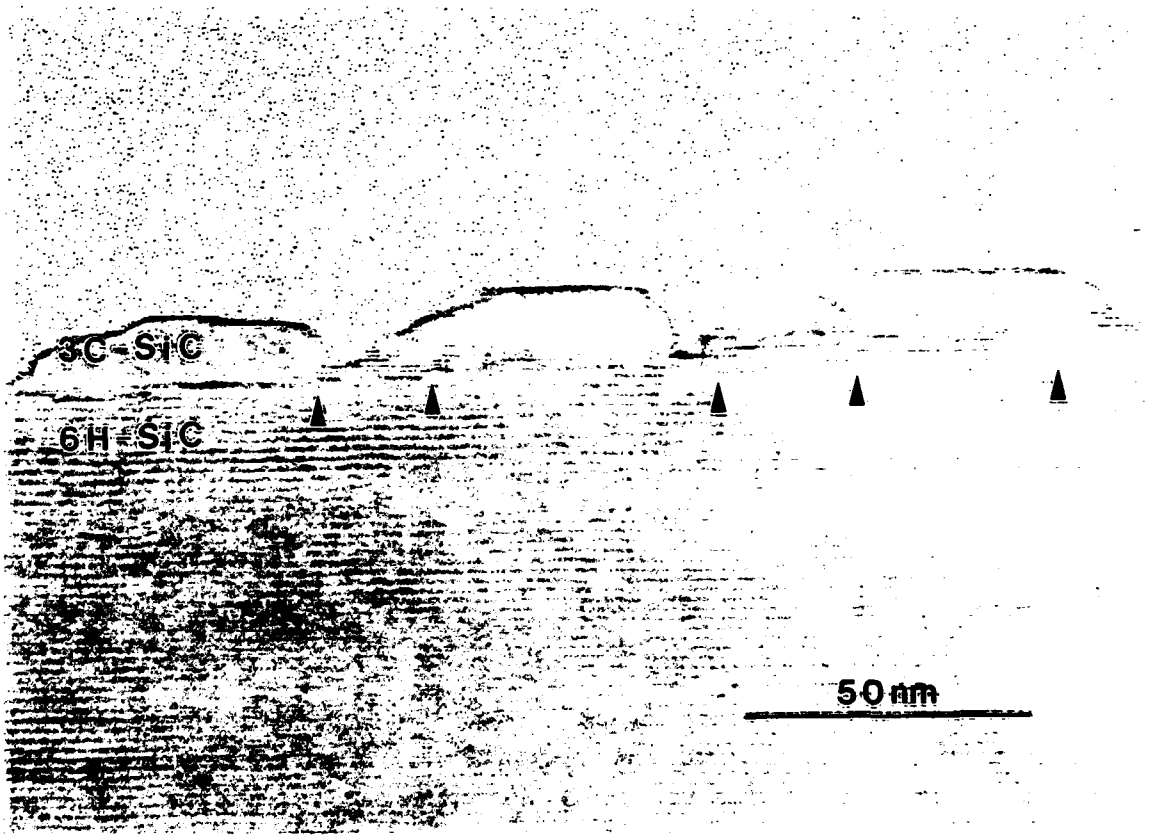

Figure 6. High-resolution TEM micrograph of 3C-SiC regions and vicinal 6H-SiC (0001) substrate. Sample was grown at 1050°C using 2.0 sccm C_2H_4 and 0.5 sccm Si_2H_6. Steps on the 6H-SiC substrate surface are denoted by arrows.

areas, adjacent regions coalesce above the steps. The areas of coalescence were much more defective than the remainder of the film.

The evidence presented in Figure 6 indicates that within the ranges of conditions employed in this study, nucleation on vicinal 6H-SiC substrates occurs on terraces between steps resulting in 3C-SiC(111). In the accepted model, independently proposed by Kong et al.[5] and Kuroda et al.[6], the density and orientation of the surface steps determine the resultant SiC polytype. If few steps are present, as in the case of nominally on-axis SiC, growth conditions determine the resultant polytype and 3C-SiC is usually formed. If there exists a high density of [11$\bar{2}$0] surface steps, then these steps serve as a template for SiC growth and the stacking sequence of the 6H polytype is preserved. However, in our studies, the kinetics of surface migration are sufficiently decreased as a result of the reduced substrate temperature that β-SiC nucleates on the terraces rather than at the surface steps.

The surface treatment prior to growth also differed between our MBE and the previous CVD studies. These differences may have affected the resultant SiC polytype and the density of defects such as DPBs. Two groups of researchers have observed that variation in surface treatment prior to growth can reduce or virtually eliminate DPBs formed on the resultant film[11,12]. This difference in surface treatment may also cause the resultant polytype to be 3C rather than 6H. Studies concerned with this topic are ongoing in the authors' laboratory.

In summary, monocrystalline films of β(3C)-SiC(111) were grown on 3-4° off-axis α(6H)-SiC(0001) substrates at 1050-1250°C by GSMBE using C_2H_4 and Si_2H_6 at a flow rate ratio of 2:1. High-resolution TEM showed that nucleation and growth occurred on the terraces between closely-spaced substrate steps as a result of the reduction in the kinetics of surface migration of the reactive species relative to that found in CVD processes where α(6H)-SiC is normally deposited.

ACKNOWLEDGEMENTS

The authors acknowledge the support of this research by the Office of Naval Research under Grant #N00014-88-K-0341. We also express our appreciation to Applied Science and Technology, Inc., Woburn, MA for the ECR source, and to Cree Research, Inc., Durham, NC for the vicinal 6H-SiC substrates.

REFERENCES

1. R. F. Davis, J. W. Palmour, and J. A. Edmond, Diamond and Related Materials **1**, 109 (1992).
2. H. S. Kong, J. T. Glass, and R. F. Davis, Appl. Phys. Lett. **49**, 1074 (1986).
3. K. Shibahara, N. Kuroda, S. Nishino, and H. Matsunami, Jpn. J. Appl. Phys. **26**, L1815 (1987).

4. H. S. Kong, B. L. Jiang, J. T. Glass, G. A. Rozgonyi, and K. L. More, J. Appl. Phys. **63**, 2645 (1988).
5. H. S. Kong, J. T. Glass, and R. F. Davis, J. Appl. Phys. **64**, 2672 (1988).
6. N. Kuroda, K. Shibahara, W. Yoo, S. Nishino, and H. Matsunami, in *Extended Abstracts of the 19th Conf. on Solid State Devices and Materials*, (Business Center for Academic Societies, Tokyo, 1987) p. 227.
7. S. Kaneda, Y. Sakamoto, T. Mihara, and T. Tanaka, J. Cryst. Growth **81**, 536 (1987).
8. T. Yoshinobu, H. Mitsui, I. Izumikawa, T. Fuyuki, and H. Matsunami, Appl. Phys. Lett. **60**, 824 (1992).
9. L. B. Rowland, R. S. Kern, S. Tanaka, and R. F. Davis, in *Proceedings of 4th International Conference on Amorphous and Crystalline Silicon Carbide and Related Materials*, (Springer-Verlag, Berlin, 1992) (in press).
10. J. C. Bravman and R. Sinclair, J. Electron Microsc. Tech. **1**, 53 (1987).
11. J. A. Powell, D. J. Larkin, L. G. Matus, W. J. Choyke, J. L. Bradshaw, L. Henderson, M. Yoganathan, J. Yang, and P. Pirouz, Appl. Phys. Lett. **56**, 1353 (1990).
12. Y. C. Wang, M. S. Thesis, North Carolina State University, 1991.

III. Chemical and Electrical Mechanisms in Titanium, Platinum, and Hafnium Contacts to Alpha(6H) Silicon Carbide

A. Introduction

In metal-semiconductor contacts a critical quantity which describes the relationship between the two materials is the Schottky barrier height (SBH), Φ_B. In general it is this property which best indicates the electrical characteristics of the contact. For an ohmic contact, in which the current is both linear and symmetric for positive and negative voltages, one would expect a small or negative SBH. On the other hand, for a good rectifying contact, in which current flows only under forward bias, one would expect a relatively large SBH.

Because the SBH is such an important parameter in terms of defining the ohmic or rectifying characteristics of a particular contact, it is very important to understand how it is determined. In the ideal case the SBH is defined by the Schottky-Mott limit, or (for an n-type semiconductor) the difference between the metal workfunction and the electron affinity of the semiconductor. However, there are many factors which can cause non-ideal relationships, and hence deviations from this rule. J. Pelletier et al. [1] have reported Fermi level pinning in 6H-SiC attributed to intrinsic surface states, suggesting little dependence of barrier height on the workfunction of the metal. In addition, L.J. Brillson [2,3] predicts the pinning rate to be higher for more covalently bonded materials.

Alpha (6H)-SiC is a particular polytype of silicon carbide, a wide bandgap semiconductor, being used in many high-power, -temperature, -frequency, and radiation hard electronic and opto-electronic devices. The future development of SiC device technology depends on, and may in fact be limited by, the ability to form good ohmic and Schottky contacts. In this study a multi-aspect approach is used in order to try to understand what determines the SBH of metal/6H-SiC contacts. Electrical characteristics of Ti, Pt, and Hf contacts before and after annealing will be discussed along with some of the interface phase chemistry and structure.

B. Experimental Procedures

Vicinal single crystal, nitrogen-doped, n-type (10^{16} - 10^{18} cm^{-3}) substrates of 6H-SiC (0001) containing 0.5-0.8 μm thick, nitrogen-doped (10^{16} cm^{-3}) homoepitaxial films were provided by Cree Research, Inc. The Si-terminated (0001) surface, tilted 3°-4° towards [11$\bar{2}$0] was used for all depositions and analyses.

For processing Ti contacts substrates were cleaned in sequence using a 10 min. dip in an ethanol / hydrofluoric acid / water (10:1:1) solution and a thermal desorption in ultra-high vacuum (UHV) (1 - 5×10^{-10} Torr). All processing steps were the same for Pt and Hf contacts, except 10% HF in deionized water was substituted for the wet chemical clean. A

resistive graphite heater was used to heat the substrates at 700°C for 15 min.

A Riber x-ray photoelectron spectroscopy (XPS) system, consisting of a Mac2 semi-dispersive electron energy analyzer and accessible by UHV transfer from the heating station and deposition chamber, was used to monitor surface chemistry and band bending. A Mg anode was used at 1.2 eV resolution for obtaining valence structure and 0.8 eV resolution for core level data.

The metals were deposited onto unheated substrates by electron beam evaporation (base pressure < 2×10^{-10} Torr). For films less than or equal to ~10 nm, a deposition rate of ~1 nm/min was used. For thicker films the rate was increased to 2 - 3 nm/min after deposition of the first 10 nm.

For electrical characterization vertical contact structures consisting of 500 μm and 750 μm diameter circular contacts of 100 nm thickness were created by depositing the metal through a Mo mask in contact with the SiC epitaxial layer, leaving a patterned metal film. Conductive liquid Ag served as the large area back contact. All subsequent annealing was done in UHV. Current-voltage (I-V) measurements were taken with a Rucker & Kolls Model 260 probe station in conjunction with an HP 4145A Semiconductor Parameter Analyzer. Capacitance-voltage (C-V) measurements were taken with a Keithley Model 5956 Package 82 Simultaneous CV System in conjunction with an HP vector PC-308. The contact structures were the same as above. Measurements were taken at a frequency of 1 MHz.

All metal/SiC samples were prepared in cross-section for TEM analysis. High resolution images were obtained with an ISI EM 002B operating at 200 kV. Analytical electron microscopy was performed with a Philips 400 FEG, installed with Gatan 607 parallel electron energy loss spectrometer, operated at 100 kV.

C. Results

Ti Contacts. In this section electrical characteristics, particularly the Schottky barrier height (SBH) measured by I-V, C-V, and XPS techniques, of unannealed and annealed Ti films deposited on 6H-SiC will be presented along with the identification of phases formed in the reaction zone. The room temperature deposition of Ti on (0001) SiC resulted in epitaxial films [4]. Both Ti (a = 2.95 Å, c = 4.68 Å) and 6H-SiC (a = 3.08 Å, c = 15.11 Å) have hexagonal crystal structures, corresponding to a 4% lattice mismatch in the (0001) basal plane.

Current-voltage measurements of as-deposited Ti contacts were found to be rectifying with low ideality factors and with typical leakage currents of 5×10^{-7} A/cm^2 at -10 V [4]. After annealing at 700°C for 20 minutes, the leakage increased; however, after further annealing up to 60 minutes the characteristics in terms of leakage and ideality factors again improved.

The low ideality factors were taken as evidence that thermionic emission theory may be applied for calculating the SBH [5]. For values of applied voltage greater than 3kT/q, the

current density can be expressed as

$$J = J_0 \exp\left(\frac{qV}{nkT}\right),$$

where J_0 is the extrapolated current at zero voltage, and n is the ideality factor. The SBH can then be determined from the equation

$$\Phi_B = \frac{kT}{q} \ln\left(\frac{A^{**}T^2}{J_0}\right),$$

where A** is the effective Richardson constant. An SBH of 0.85 eV was calculated for unannealed Ti contacts. This barrier was found to increase to 0.95 eV after annealing at 700°C for 60 minutes.

Barrier heights were also determined from capacitance-voltage measurements. By plotting $1/C^2$ vs. V the barrier height can be determined from the equation

$$\Phi_B = V_i + V_n + \frac{kT}{q},$$

where V_i is the voltage intercept ,and V_n is the difference between the conduction band and the Fermi level. Figure 1 shows $1/C^2$ vs. V of an as-deposited Ti/SiC contact biased from 0 to -2 V. Extrapolating the linear region gives an intercept of 0.67 V, indicating a SBH of 0.88 V. Similarly, a SBH of 1.04 V was calculated for annealed contacts.

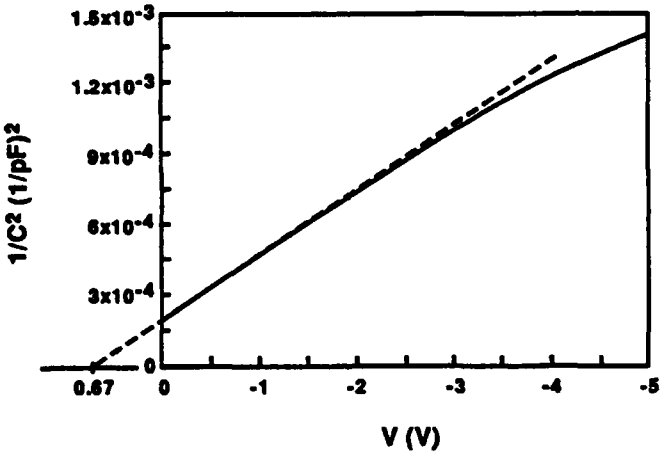

Figure 1. $1/C^2$ vs. V of as-deposited Ti/SiC (contact area = 2.0×10^{-3} cm^2) $\Phi_B \cong 0.88$ V.

X-ray photoelectron spectroscopy, typically used for chemical analysis of surfaces, was a third technique used for calculating the SBH of Ti on SiC. In this technique photoelectrons are ejected from the near surface (~20 Å) region on which Mg Kα (1253.6 eV) or Al Kα

(1486.6 eV) x-rays are focused. The binding energy is determined from the kinetic energy of the ejected photoelectrons. Prior to depositing any metal atoms the valence levels of the SiC surface were examined by measuring the high kinetic energy electrons (Fig. 2(a)). The top of the valence band was estimated by extrapolating the leading edge of the lowest binding energy peak. With reference to the 3.9 eV Fermi level (determined with a Au standard), the top of the valence band sits at approximately 1.8 eV. Since the SiC epitaxial layer (bandgap = 2.86 eV) is doped n-type (10^{16} cm^{-3}), these results indicate that the bands bend upward at the semiconductor surface (E_C–$E_F \approx 1.1$ eV).

Core level peaks were also obtained from the SiC surface and the Ti/SiC interface after depositing Ti in 2 Å to 4 Å increments. The Si 2p, C 1s, and Ti $2p_{3/2}$ and $2p_{1/2}$ doublet peaks at various stages in the series are shown in Figure 2 (b), (c), and (d), respectively. Subtracting the 3.9 eV workfunction of the analyzer, the silicon and carbon peaks prior to deposition of Ti are located at 100.5 and 282.7 eV, respectively, the expected binding energies for Si-to-C bonding [6]. After depositing approx. 4 Å Ti a shoulder on the low binding energy side of the C peak begins to form and is attributed to TiC bonding [7,8]. The fact that no shifts were detected in the Si peak or the portion of the C peak due to C-Si bonding indicates that there is no change in band bending; therefore, the barrier height is estimated to be equal to 1.1 eV.

The Ti/SiC interface was also studied with high resolution transmission electron microscopy (HRTEM) and is reported in more detail elsewhere [9]. After annealing at 700°C for 20 minutes, the reaction zone was found to consist of a very thin layer of cubic TiC_{1-x} in contact with the SiC and a layer of orthorhombic Ti_5Si_3 with TiC_{1-x} particles at the Ti side of the interface. After annealing for 60 minutes, the width of the reaction zone did not increase, but the TiC_{1-x} particles disappeared. The position of layers comprising the interface is SiC / TiC_{1-x} / Ti_5Si_3 / Ti. The lattice parameter of TiC_{1-x} varied by approximately 2% along the SiC interface.

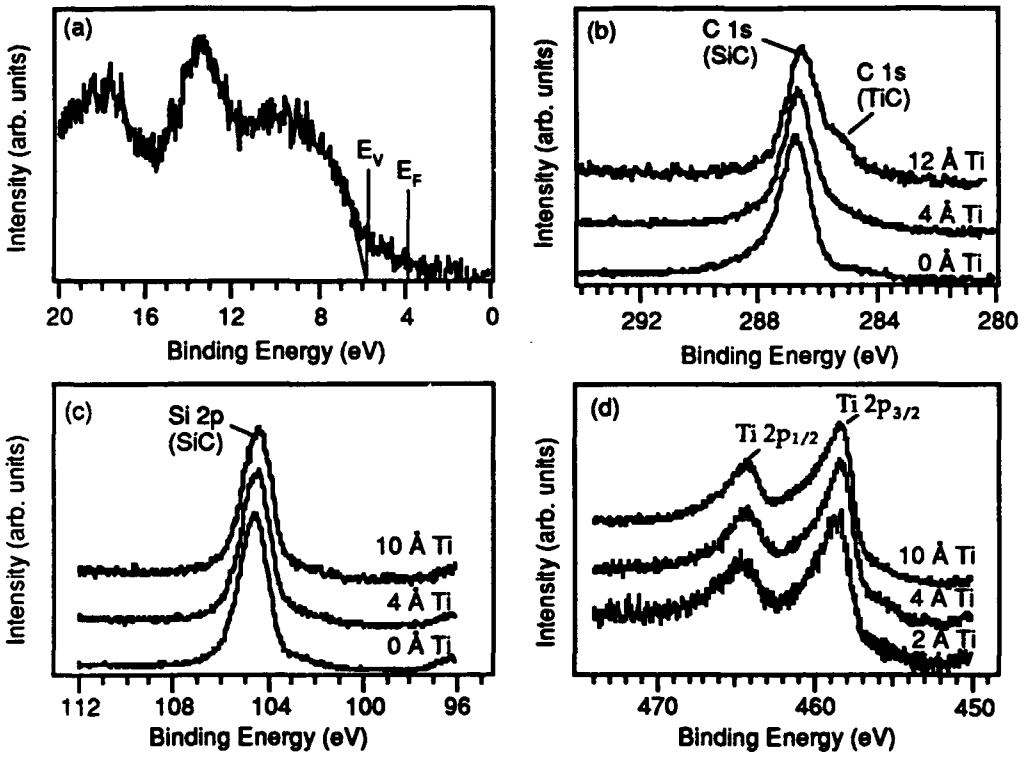

Figure 2. XPS spectra of (a) valence levels of chemically-cleaned SiC surface and (b) C 1s, (c) Si 2p, and (d) Ti 2p peaks after depositing various thin layers of Ti.

Pt Contacts. Platinum contacts deposited at room temperature formed Schottky contacts to SiC with low leakage currents and low ideality factors (Fig 3). The leakage at -10 V was typically 5 x 10^{-8} A/cm^2, and the ideality factors were consistently between 1.02 and 1.06. Using the procedure outlined above, a barrier height of 1.06 eV was calculated from I-V measurements.

These contacts were annealed from 450°C to 750°C in 100 °C increments for 20 minutes at each temperature. Figure 4 shows an interesting trend through this annealing series, throughout which the ideality factors and leakage currents remained low; the SBH increased with anneal temperature to 1.26 eV. These results are similar to those reported by Papanicolaou et al. [10] in which the SBH of Pt on β-SiC increased from 0.95 eV for as-deposited contacts to 1.35 eV after annealing at 800°C.

Initial investigation of the Pt/SiC interface with HRTEM has been performed. The unannealed films are polycrystalline with a grain size of 10 nm. Observation of the 650°C annealed interface revealed an increase of the average grain size to 80 nm. After annealing at 750°C, the reaction zone consisted of a 12 nm amorphous region with some crystalline regions apparently nucleating at ledges in the SiC surface.

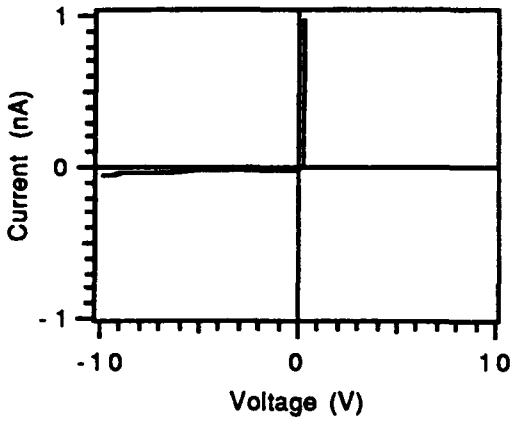

Figure 3. I vs. V of Pt/SiC (contact area = 2.0 x 10^{-3} A/cm^2).

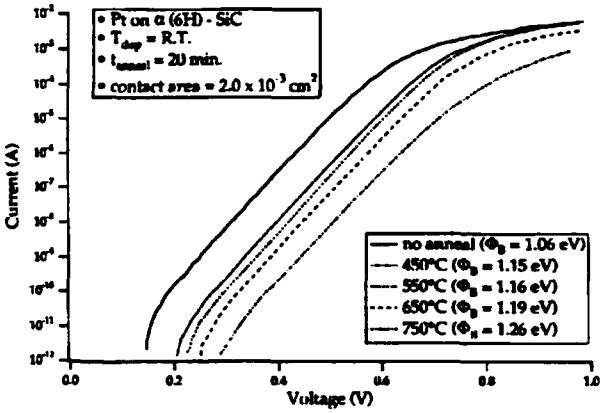

Figure 4. Log I vs. V of Pt/SiC.

Hf Contacts. Current-voltage measurements of as-deposited and annealed hafnium contacts also displayed rectifying characteristics and low ideality factors. The as-deposited contacts produced typical leakage currents of 2.5 x 10^{-7} A/cm^2 at -10 V, while annealing at 700°C for 20 minutes resulted in a reduction of the leakage to 4.0 x 10^{-8} A/cm^2. Upon further annealing, the leakage currents increased.

Concomitant with the observable variation in the reverse characteristics with annealing time, the calculated SBH was found to vary. The 0.97 eV SBH for the unannealed contacts increased to 1.01 eV after the 20 min. anneal and then successively decreased to 0.93 eV and 0.86 eV for the 40 min. and 60 min. anneals, respectively. Qualitatively, the leakage current appears to vary inversely with the height of the barrier, as would be expected.

Initial investigation of these interfaces with HRTEM was performed. Although Hf (a = 3.19 Å, c = 5.05 Å) also has a hexagonal crystal structure with a <4% lattice mismatch with the (0001) basal plane of SiC, epitaxial growth did not occur. Preliminary investigation of Hf/SiC interfaces after annealing at 700°C has not revealed the formation of any new phases.

D. Discussion

The measured and predicted SBH's have been compared for the three metals studied here with n-type SiC (Table 1). The measured values were taken from I-V measurements as reported above, while the predicted values were calculated from the workfunctions of the respective metals. Although the theoretical values vary from 0.52 eV to 2.27 eV, a 1.75 eV range, the measured values vary by less than 0.2 eV.

Table 1. Measured and theoretical Schottky barrier heights for as-deposited Ti, Pt, and Hf on n-type 6H-SiC.

Metal	Φ_B^{I-V} (eV)	Φ_B^{th} (eV)
Ti	0.85	0.95
Pt	1.02	2.27
Hf	0.97	0.52

The XPS valence spectrum of the SiC surface (Fig. 2(a)) provides additional insight regarding energy band relationships. The fact that the bands bend upward at the surface without a metal overlayer indicates that surface states are present. It is unknown at this time whether these states are intrinsic or extrinsic (i.e. surface impurities). However, the surface states appear to affect charge transfer between the metals and SiC, and hence largely control the SBH.

There are additional changes in the SBH's resulting from annealing the interfaces. These changes might be expected since the original surface has reacted to form new phases. In the Ti/SiC system the phase in contact with SiC after annealing at 700°C is titanium carbide. In fact, Ti-C bonding was detected in the C 1s peak (Fig. 2(b)) after deposition of approximately 4 Å of Ti at room temperature.

The formation of TiC_{1-x} and Ti_5Si_3 in the Ti/SiC system at higher temperatures (1200 - 1500°C) has been reported by others [11-13]. At 700°C the results seem to indicate that the kinetics of forming TiC are faster than that of forming Ti_5Si_3, resulting in the TiC phase being adjacent to the SiC.

Because the TiC phase forms a continuous layer adjacent to the SiC, that phase should determine the contact characteristics after 700°C annealing. However, the low workfunction (~2.6 eV [14]) determined experimentally for single crystal TiC would predict ohmic behavior. The non-ohmic behavior may be due to one or more of the following reasons: (1) unknown increase in the workfunction with the non-stoichiometry, (2) metal-induced gap states, and (3) incomplete removal of surface states.

E. Conclusions

A combination of techniques was used to study the electrical, chemical, and/or structural

properties of Ti, Pt, and Hf contacts to n-type 6H-SiC. All of these contacts were rectifying with ideality factors less than 1.1. Although the workfunctions would predict a >1.5 eV range in SBH for the as-deposited contacts, I-V and C-V measurements indicate a <0.2 eV variation between metals. In addition, an XPS valence spectrum of the SiC surface indicates that the Fermi level lies approx. 1.8 eV above the top of the valence band, relatively near the middle of the bandgap. Pinning of the Fermi level in the bandgap would explain the small dependence of the SBH on metal workfunction.

Although the SBH for Pt contacts was found to increase with annealing temperature, there was not much change observed in Ti contacts after annealing at 700°C. The reaction zone was found to consist of Ti_5Si_3 and a TiC_{1-x} layer adjacent to the SiC. Readers are referred to J. S. Bow et al. [9] for more discussion on this subject.

F. Future Research Plans/Goals

Efforts will be continued to gain a cohesive understanding of what determines the SBH's of Ti, Pt, and Hf contacts to 6H-SiC. Because the results of the experiments performed on these metal/SiC systems imply that the Fermi level is pinned at the SiC surface, comparison to other cleaning techniques is planned in the immediate future. Similar XPS experiments will be performed to determine the location of the Fermi level. If the bands at the surface are found to be flat (i.e. Fermi level is unpinned), SBH's will be remeasured and compared previous values.

Two other metal contacts, Co and Sr, chosen for this study will also be analyzed in terms of electrical, chemical, and structural characteristics. Because of its low workfunction, it is proposed that Sr will form an ohmic contact if the Fermi level is unpinned. In addition, with comparison to Ni, Co also may form an ohmic contact after high temperature annealing. These metal / SiC systems will then be compared in terms of their ohmic or rectifying characteristics.

G. References

1. J. Pelletier, D. Gervais, and C. Pomot, J. Appl. **55** (1984) 994.
2. L. J. Brillson, Phys. Rev. B, **18** (1978) 2431.
3. L. J. Brillson, Surf. Sci. Rep., **2** (1982) 123.
4. L. M. Spellman, R.C. Glass, R.F. Davis, T.P. Humphreys, H. Jeon, R.J. Nemanich, S. Chevacharoenkul, and N. R. Parikh, Mat. Res. Soc. Symp. Proc., **221** (1991) 99-104.
5. See for example, E. H. Rhoderick and R. H. Williams, *Metal-Semiconductor Contacts*, 2nd Ed. (Clarendon Press, Oxford, 1988); S. M. Sze, *Physics of Semiconductor Devices*, 2nd Ed.(John Wiley & Sons, New York, 1981); H. K. Henisch, *Semiconductor Contacts* (Clarendon Press, Oxford, 1984).
6. K. L. Smith and K. M. Black, J. Vac. Sci. Technol. A, **2** (1984) 744.
7. L. Ramquist, K. Hamrin, G. Johansson, A. Fahlman, and C. Nordling, J. Phys. Chem. Solids, **30** (1965) 1835.
8. H. Ihara, Y. Kumashiro, A. Itoh, and K. Maeda, Jap. J. Appl. Phys., **12** (1973) 1462.

9. J. S. Bow, M. J. Kim, R. W. Carpenter, L. M. Porter, and R. F. Davis, Mat. Res. Soc. Symp. Proc. (1992), to be published.
10. N. A. Papanicolaou, A. Christou, and M. L. Gipe, J. Appl. Phys. **65** (1989) 3526.
11. M. Backhaus-Ricoult, Acta-Scripta Met. Proc., **4** (1989) 79.
12. S. Sambasivan and W.T. Petusky, J. Mater. Res., **7** (1992) 1473.
13. C. E. Bruckl, AFML Tech. Rep., AFML-TR-65-2, Pt. II, Vol. VII, Air Force Materials Laboratory, Wright Patterson Air Force Base, OH (1966).
14. K. Senzaki and Y. Kumashiro, Bull. Electrotech. Lab. Jpn. **41** (1977) 593.

IV. Epitaxial Growth of AlN by Plasma-Assisted Gas-Source Molecular Beam Epitaxy

A Communication
Submitted for Consideration for Publication
to
The Journal of Materials Research

L. B. Rowland*, S. Tanaka, R. S. Kern and Robert F. Davis
Department of Materials Science and Engineering
North Carolina State University
Box 7907
Raleigh, North Carolina 27695-7907

November, 1992

ABSTRACT

Monocrystalline AlN(0001) films with few defects were deposited on vicinal α(6H)-SiC(0001) wafers via plasma-assisted gas-source molecular beam epitaxy within the temperature range of 1050–1200°C. The Al was thermally evaporated from an effusion cell. An electron cyclotron resonance plasma source was used to produce activated nitrogen species. Growth on vicinal Si(100) at 900–1050°C resulted in smooth, highly oriented AlN(0001) films.

*Present Address
Naval Research Laboratory, Code 6861
4555 Overlook Av., SW
Washington, DC 20375-5320

Aluminum nitride possesses a direct bandgap of 6.28 eV at 300 K [1], a melting point in excess of 2275 K [2] and a thermal conductivity of 3.2 W/cm·K [3]. As such, it is a candidate material for high-power and high-temperature microelectronic and optoelectronic applications with the latter employment being particularly important in the ultraviolet region of the spectrum [1]. This material also has the highest reported surface acoustic wave velocity (Raleigh V_R=6–6.2 km/s, V_L=11-12 km/s [4]-[6]) for any material and a substantial electromechanical coupling coefficient (to 1% [7]). These properties strongly indicate that superior surface acoustic wave devices, operational in aggressive media and under extreme conditions both as sensors for high temperatures and pressures and as acousto-optic devices can be developed [8-10]. However, progress regarding these (and other) applications is hampered by the lack of good single crystal material. The primary objective of the research reported below has been to address this issue via the fabrication of thin films of this material via molecular beam epitaxy (MBE) techniques.

In previous studies, mono- and polycrystalline films of AlN have been grown by chemical vapor deposition (CVD) using NH_3 and $Al(CH_3)_3$ or $AlCl_3$ on α(6H)-SiC [11], sapphire [1,9,12], and Si [13-15]. Chu et al. [11] obtained smooth monocrystalline AlN layers to a thickness of 25 μm on α(6H)-SiC{0001} substrates by chemical vapor deposition (CVD) from 1200-1250°C. A high density of defects in these AlN films was revealed by chemical etching. In general, films grown on sapphire and Si substrates possessed a rougher morphology than those grown on α(6H)-SiC. This occurred very likely because the difference in lattice parameters between AlN and SiC is substantially less than between AlN and sapphire or AlN and Si.

Gas source MBE using electron beam evaporated Al and NH_3 [16] or thermally evaporated Al and plasma-derived activated nitrogen species [17] has also been used for single crystal AlN growth. Yoshida et al. [16] obtained single crystal AlN using an Al effusion cell and NH_3 at 1000-1200°C on Si(111) and Al_2O_3(0001) and (01$\bar{1}$2) and obtained growth rates of up to 1 μm/hr. They contended that their films were much smoother than CVD-grown material and rivaled bulk single crystal AlN. Sitar et al. [17] used an electron cyclotron resonance (ECR) plasma for decomposition of N_2 and Al and Ga effusion cells for growth of AlN/GaN superlattices by plasma-assisted, gas source (PAGSMBE) on α(6H)-SiC (0001) and Al_2O_3 (0001) at 600°C. The thickness range of the AlN layers was 0.5–20nm, as determined by cross-sectional transmission electron microscopy (TEM). However, the properties of the individual AlN layers were not examined.

The approach taken in the present research has also been to use PAGSMBE to achieve surface reactions involving only Al and N in order to minimize the potential for unintentional impurity contamination from the p- and n-type dopants of C and O, respectively. The AlN films were grown on vicinal Si(100) wafers oriented 3.5 ± 0.5° towards [011] at 900-1050°C

and vicinal α(6H)-SiC (0001) oriented 3-4° towards [11$\bar{2}$0] at 1050-1200°C in a PAGSMBE system described previously [18]. These temperatures are higher than necessary for the formation of single crystal AlN. However, they were employed to match the growth temperatures previously determined to be necessary to achieve single crystal films of SiC on Si(100) [18-20] and α(6H)-SiC(0001) substrates [21,22].

Silicon(100) substrates were chemically cleaned using the following steps: (1) H_2SO_4 at 70°C for 5 min, (2) deionized water for 1 min, (3) 1:1 solution (by volume) of NH_4OH and 50% H_2O_2 at 70°C for 5 min, (4) deionized water for 1 min, (5) dip in 10% HF at room temperature, and (6) 2 min rinse in deionized water. Silicon carbide substrates were only subjected to cleaning steps (5) and (6) prior to introduction to the growth system. Thermal desorption of all substrates was also conducted at the growth temperature for 5 min prior to deposition to remove any remaining hydrocarbon and/or oxide contamination. An effusion cell was used for the evaporation of Al (99.999% pure). Reactive nitrogen species were produced via decomposition of N_2 (99.999% pure) in a compact electron cyclotron resonance (ECR) plasma source (Applied Science and Technology, Inc.). The pressure of the introduced N_2 was 1.2-1.5 x 10^{-4} torr. The microwave power supplied to the ECR was 100 W for all depositions.

The crystallography and surface character on the films were initially studied *in situ* using reflection high-energy electron diffraction (RHEED). The microstructure of the final growth surface was investigated using field-emission scanning electron microscopy (SEM). The orientation of the films grown on Si was determined via x-ray diffraction. A more in-depth examination of the crystallinity and the nature and distribution of the line and planar defects in the films deposited on 6H-SiC was conducted using high-resolution transmission electron microscopy (HRTEM). The composition of the films, including any significant impurities, was determined using an Auger electron microprobe.

Figure 1 shows the RHEED patterns ([11$\bar{2}$0] azimuth) of AlN films grown on the 6H-SiC (0001) substrates at (a) 1200°C, (b) 1100°C and (c) 1050°C. These patterns indicate that all the films possess the wurtzite structure and are monocrystalline.

The growth rate versus temperature was essentially constant for a given Al flux. Conversely, changes in the AlN growth rate corresponded directly to changes in the Al flux. A constant Al source temperature and, consequently, a constant Al flux were used at the the three temperatures of growth. An excess of activated nitrogen was present under all conditions. A constant growth rate of ≈0.40 nm/min was obtained at these temperatures.

Scanning Auger analysis of these films detected only Al and N except in a 2 nm surface region where the native oxide (and very likely the hydroxide) had formed during exposure to air. The stoichiometry of these films was very close to that obtained from analysis of high-purity, hot-pressed polycrystalline AlN. Figure 2 shows a HRTEM image of a thin AlN layer

(a)

(b)

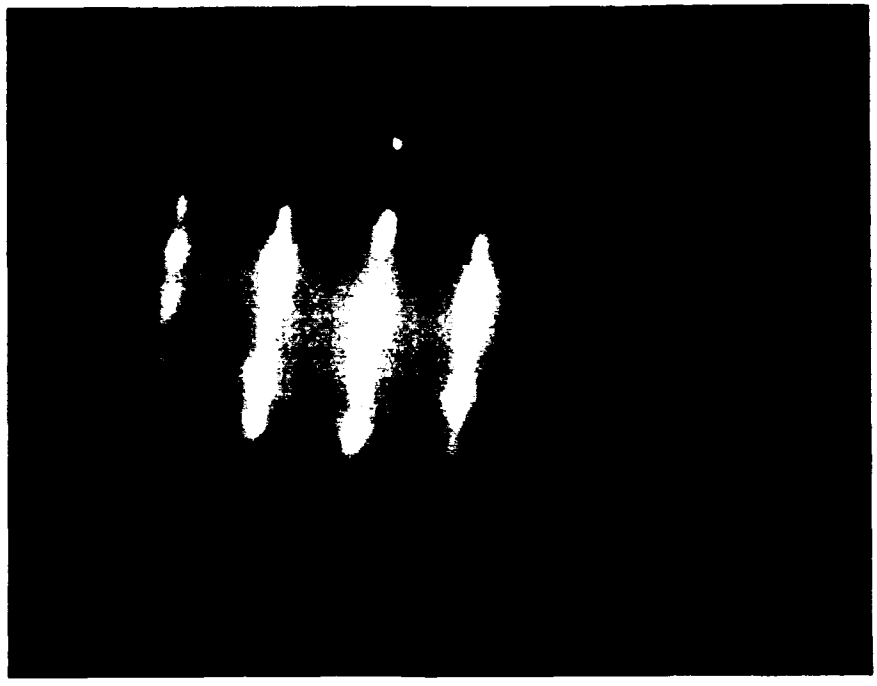

Figure 1. RHEED patterns ([11$\bar{2}$0] azimuth) of AlN grown on vicinal 6H-SiC(0001) at (a) 1200°C, (b) 1100°C, and (c) 1050°C.

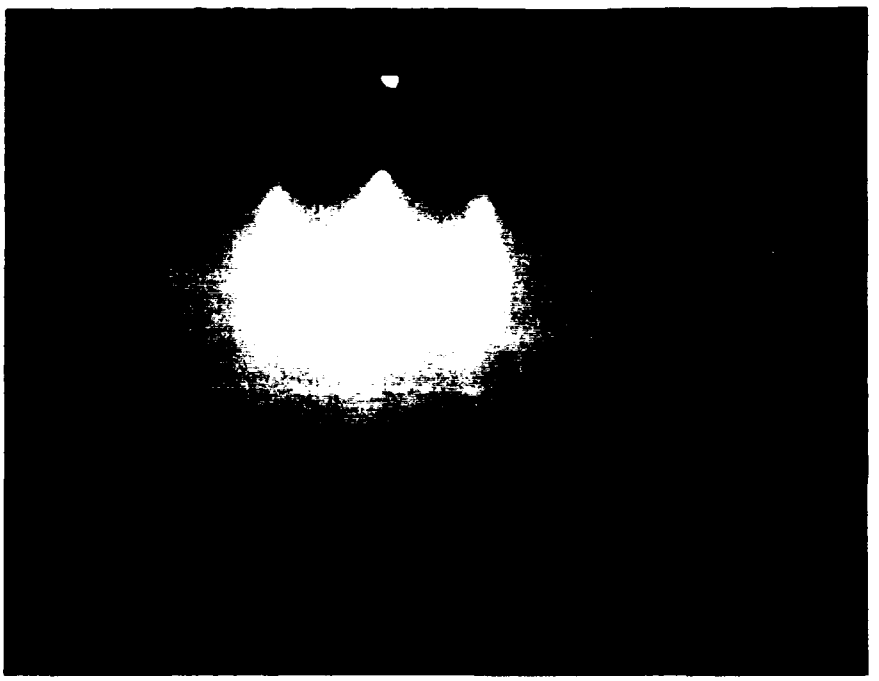

Fig. 1. (c) 1050°C.

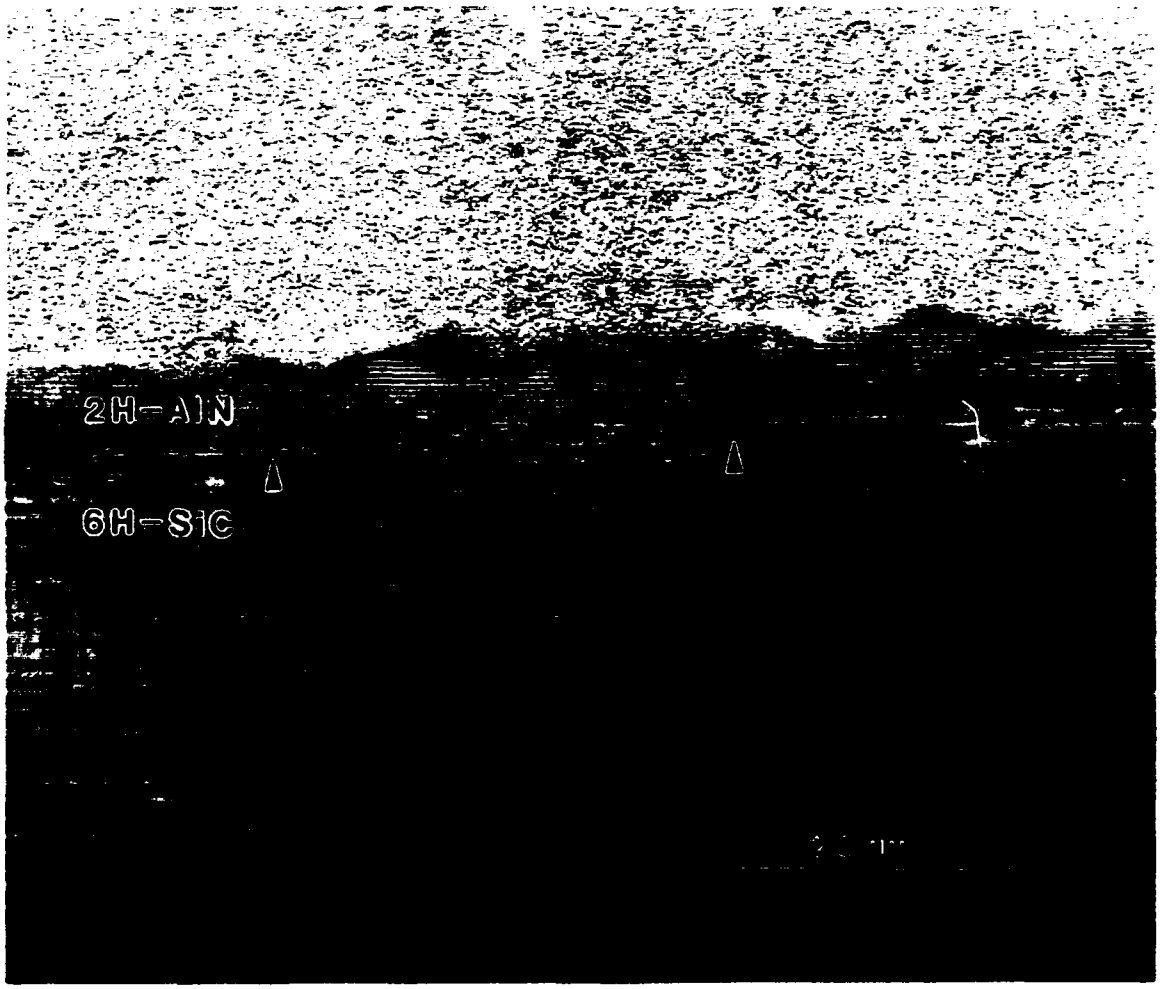

Figure 2. HRTEM micrograph of AlN film grown at 1200°C on vicinal 6H-SiC (0001). Arrows point to areas of lattice distortion in the lattice fringes of the AlN.

deposited on the 6H-SiC at 1200°C. The top surface of the AlN is rough. Few defects are visible away from the interface. At the 2H-AlN/6H-SiC interface, however, strain contrast as evidenced by distortion in the lattice fringes can be seen (denoted by arrows in Figure 2).

A further reduction in temperature to 1050°C also resulted in the deposition of single crystal AlN films (as indicated in Figure 1(c)) having an abrupt interface with the SiC substrates, but with a much smoother final surface, as shown in the SEM micrograph of Figure 3. This essentially featureless microstructure supports the RHEED results. The surface morphology was difficult to observe at much higher magnifications in the SEM due to the insulating nature of both AlN and the SiC substrate. Figure 4 shows a HRTEM image of a film grown at 1050°C capped by a monocrystalline, cubic (zincblende structure) β-SiC(111) film grown in the same experiment. The smooth AlN surface and the abrupt junction with the β-SiC are apparent. Dislocations in the AlN films occurred at surface steps in the 6H-SiC substrate and may be observed in Figure 4 (see arrow). No other defects were observed in this material. The use of nominally on-axis 6H-SiC substrates with widely spaced steps will be studied in the near future to reduce the defects present in these films.

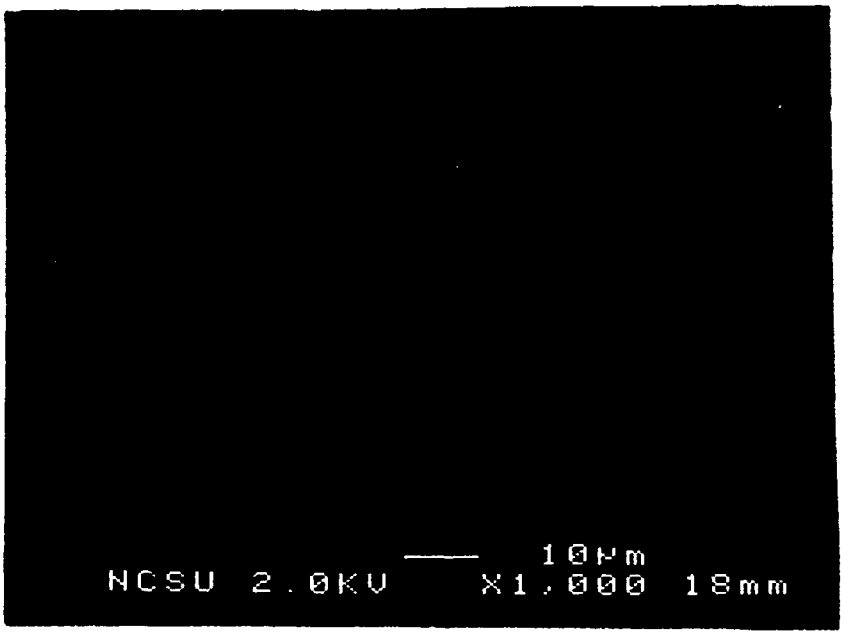

Figure 3. SEM micrograph of the surface morphology of an AlN film grown on vicinal 6H-SiC(0001) at 1050°C.

Figure 5 shows RHEED patterns of AlN layers deposited at 900 and 1050°C on Si(100) substrates. These films have the wurtzite structure and are very well-oriented. There is only a small amount of angular spread in the spots which implies that the films have a small non-epitaxial component. An X-ray diffraction scan of the film grown at 1050°C is shown in

Figure 4. HRTEM micrograph of AlN film grown at 1050°C on vicinal 6H-SiC (0001). Layer above AlN layer is 3C-SiC also grown at 1050°C using gas-source MBE. Arrow points to dislocation in the AlN film at a step on the 6H–SiC surface.

Figure 6. The single (0002) AlN peak supports the RHEED results regarding orientation. The AlN therefore grows with the closest packed plane parallel to the non-closest packed (100) plane in the Si substrate. Figure 7 shows a SEM micrograph of the grown surface at 1050°C. The film is smooth except for occasional small elongated depressions in the surface. The reason for these features has not been determined; however, they may be due to pitting of the Si surface before AlN growth. These films were extremely smooth when compared to those grown by CVD [13-15].

(a)

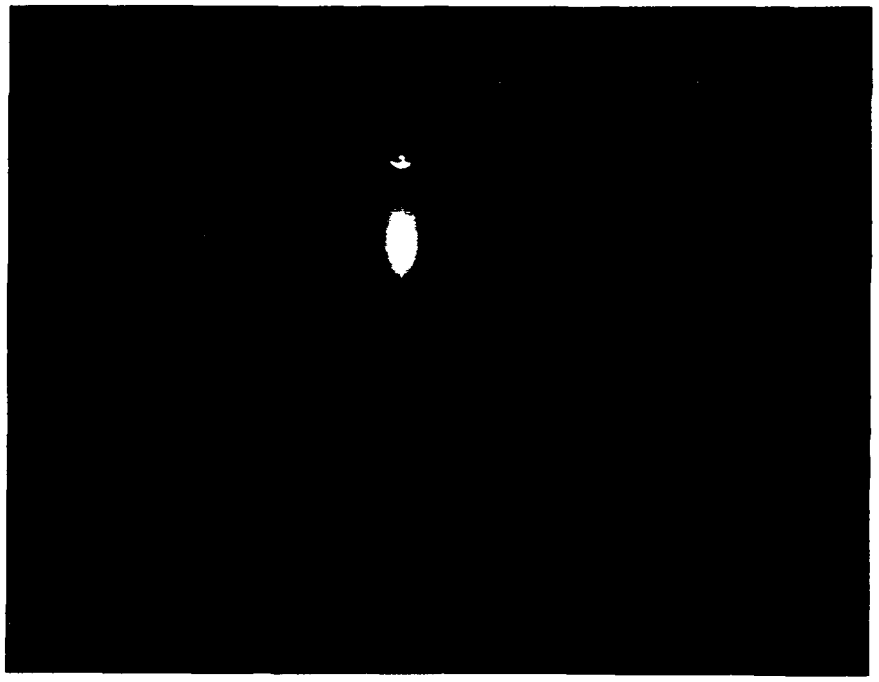

(b)

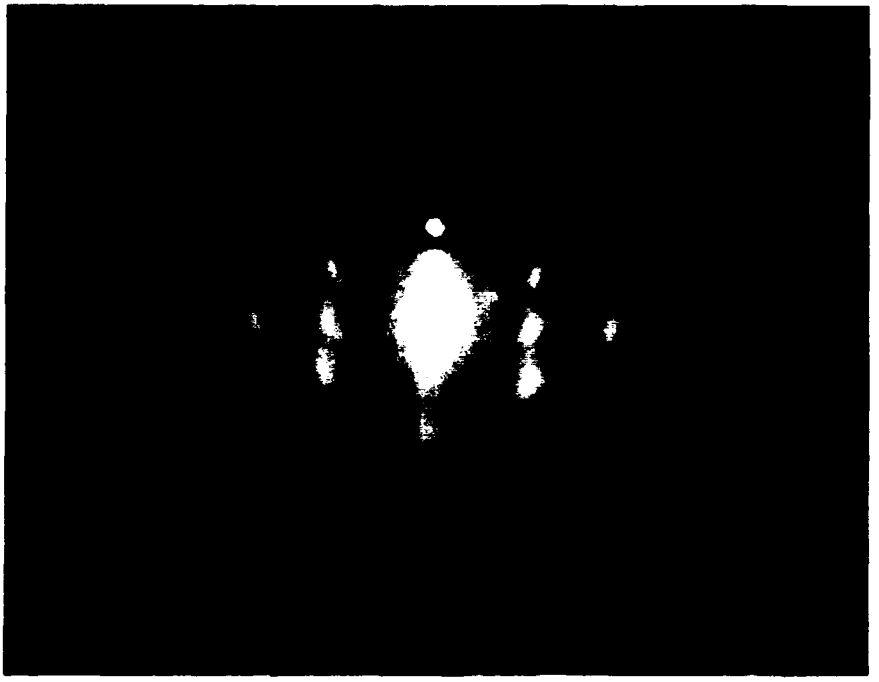

Figure 5. RHEED patterns ([11$\bar{2}$0] azimuth) of AlN films grown on vicinal Si(100) at (a) 900°C and (b) 1050°C.

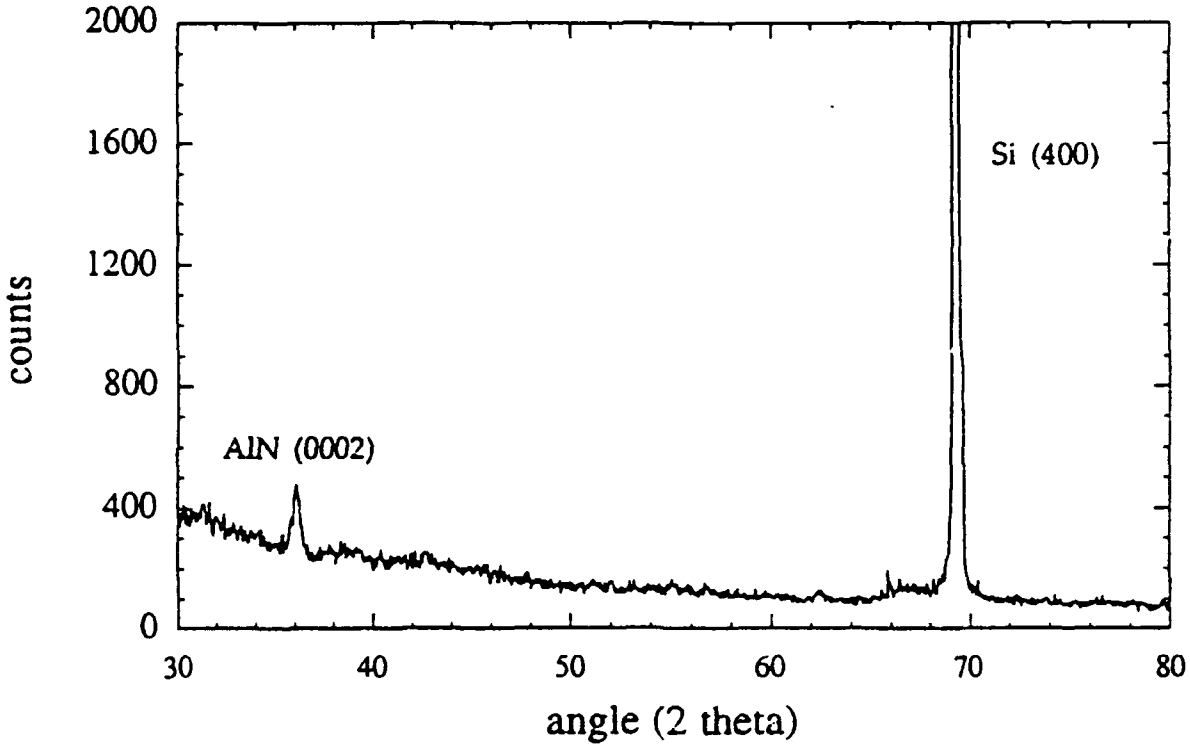

Figure 6. X-ray diffraction spectrum (CuKα) of AlN film on vicinal Si(100) at 1050°C.

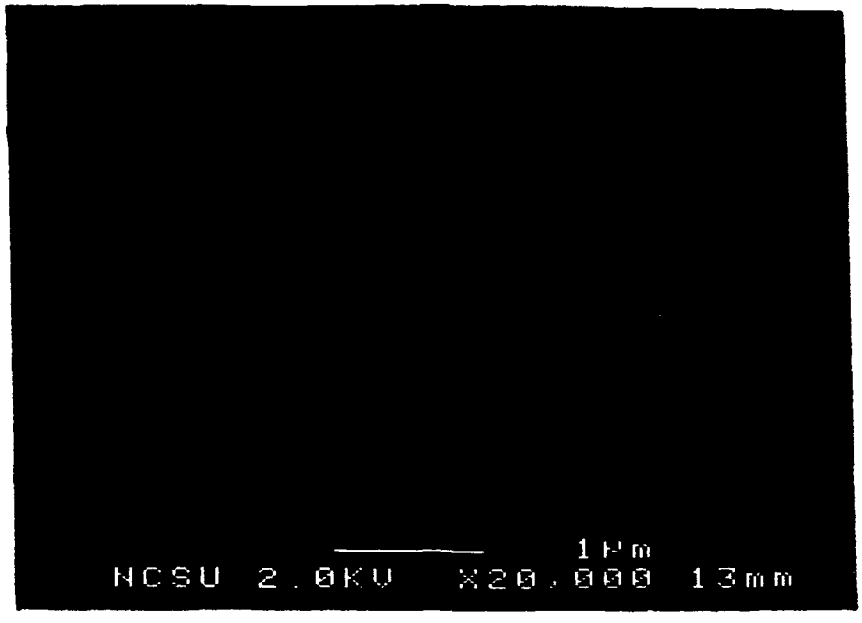

Figure 7. Scanning electron micrograph of surface morphology of AlN grown on vicinal Si(100) at 1050°C.

An orientation of AlN such as (10$\bar{1}$0) is more likely than (0001) on Si(100), based on crystallographic considerations. The latter orientation of AlN would be expected on Si (111), as the closest-packed (0001) planes of AlN contain the same general atomic arrangement. Previous reports of AlN on Si(100) are inconsistent with regard to orientational relationships. Several researchers have used trimethyaluminum and NH_3 in CVD growth on on-axis Si(100) substrates. Morita et al. [13] deposited single-crystal AlN(0001) on Si(100) at 1260°C. Yu et al. [14] grew epitaxial AlN(10$\bar{1}$0) on Si(100) at temperatures as low as 400°C. Roughening and pitting of the Si surface has been observed at temperatures as low as 800°C [24]. Thus, the roughness of the Si surface is likely to be more severe at 1260°C than at 400°C due to the evaporation of the oxide and the greater surface mobility at the higher temperature. This degradation of the surface may also explain why the films grown as a part of this study were AlN(0001) rather than AlN(10$\bar{1}$0).

In summary, monocrystalline AlN films were grown on vicinal α(6H)-SiC(0001) at 1050-1200°C using thermally evaporated Al and ECR plasma decomposition of N_2. The surfaces of the films formed at 1200°C were rough. Films grown at 1050°C were much smoother and formed an abrupt interface with the substrate. These latter films were of excellent microstructural quality when compared to those grown by CVD and reported in the literature. Highly oriented AlN(0001) films with a very smooth surface morphology were also formed on vicinal Si(100) at 1050°C. This c-axis alignment is believed to be caused by the roughness and pitting in the Si surface at the elevated growth temperatures. Doping with candidate n- and p-type impurities and the determination of the resultant properties of the AlN films will be investigated in the near future.

ACKNOWLEDGEMENTS

The authors acknowledge the support of this research by the Office of Naval Research under Grant #N00014-90-J-1427. We also express our appreciation to Applied Science and Technology (ASTeX), Inc., Woburn, MA for the ECR source, to Cree Research, Inc., Durham, NC for the vicinal α(6H)-SiC substrates, and to Ms. S. Rogers for the Auger analysis.

REFERENCES

1. W. M. Yim, E. J. Stofko, P. J. Zanzucchi, J. I. Pankove, M. Ettenberg, and S. L. Gilbert, J. Appl. Phys. **44**, 292 (1973).
2. M. G. Norton, B. C. H. Steele, and C. A. Leach, *Science of Ceramics*, **14**, 545 (1988).
3. G. A. Slack, J. Phys. Chem. Solids **34**, 321 (1973).
4. M. Kitayama, T. Fukui, T. Shiosaki, and A. Kawabata, Japan J. Appl. Phys. **22**, 139 (1982).
5. G. R. Kline and K. M. Lakin, Proc. IEEE Symp. Ultrasonics **14**, 495 (1983).

6. K. Tsubouchi, K. Sugai, and N. Mikoshiba, Proc. IEEE Symp. Ultrasonics **14**, 340 (1983).
7 M. Sano and M. Aoki, Oyo Butsuri, **52**, 374 (1983).
8. J. K. Liu, K. M. Lakin, and K. L. Wang, J. Appl. Phys **46**, 3703 (1975).
9. M. Morita, N. Uesugi, S. Isogai, K. Tsubouchi, and N. Mikoshiba, Jpn. J. Appl. Phys. **20**, 17 (1981).
10. G. D. O'Clock, Jr. and M. T. Duffy, Appl. Phys. Lett. **23**, 55 (1973).
11. T. L. Chu, D. W. Ing, and A. J. Norieka, Solid State Electron. **10**, 1023 (1967).
12. H. M. Manasevit, F. M. Erdmann, and W. I. Simpson, J. Electrochem. Soc. **118**, 1864 (1971).
13. M. Morita, S. Isogai, N. Shimizu, K. Tsubouchi, and N. Mikoshiba, Japan. J. Appl. Phys. **20**, L173 (1981).
14. Z. J. Yu, J. H. Edgar, A. U. Ahmed, and A. Rys, J. Electrochem. Soc. **138**, 196 (1991).
15. A. J. Noreika and D. W. Ing, J. Appl. Phys. **19**, 5578 (1968).
16. S. Yoshida, S. Mizawa, Y. Fujii, S. Takada, H. Hayakawa, S. Gonda, and A. Itoh, J. Vac. Sci. Technol. **16**, 990 (1979).
17. Z. Sitar, M. J. Paisley, B. Yan, R. F. Davis, J. Ruan, and J. W. Choyke, Thin Solid Films **200**, 311 (1991).
18. L. B. Rowland, R. S. Kern, S. Tanaka, and R. F. Davis, in *Proceedings of the Fourth International Conference on Amorphous and Crystalline Silicon Carbide* (Springer-Verlag, Berlin), to be published.
19. S. Kaneda, Y. Sakamoto, C. Nishi, M. Kanaya, and S. Hannai, Japan. J. Appl. Phys. **25**, 1307 (1986).
20. T. Sugii, T. Aoyama, and T. Ito, J. Electrochem. Soc. **137**, 989 (1990).
21. L. B. Rowland, R. S. Kern, S. Tanaka, and R. F. Davis, submitted for publication.
22. T. Yoshinobu, H. Mitsui, I. Izumikawa, T. Fuyuki, and H. Matusnami, Appl. Phys. Lett. **60**, 824 (1992).
23. D. J. Robbins, A. J. Pidduck, A. G. Cullis, N. G. Chew, R. W. Hardeman, D. B. Gasson, C. Pickering, A. C. Daw, M. Johnson, and R. Jones, J. Cryst. Growth **81**, 421 (1987).

V. Aluminum Nitride/Silicon Carbide Multilayer Heterostructure Produced by Plasma-Assisted Gas-Source Molecular Beam Epitaxy

Submitted for Consideration for Publication
to
Applied Physics Letters

L. B. Rowland*
R. S. Kern
S. Tanaka
Robert F. Davis

North Carolina State University
Department of Materials Science and Engineering
Box 7907
Raleigh, North Carolina 27695-7907

November, 1992

ABSTRACT

Pseudomorphic bilayer structures containing β(3C)-SiC and 2H-AlN have been grown on vicinal α(6H)-SiC(0001) homoepitaxial layers at 1050°C by plasma-assisted, gas source molecular beam epitaxy. High energy electron diffraction and cross-sectional high-resolution transmission electron microscopy showed all layers to be monocrystalline. The AlN layers were uniform in thickness. Defects in these layers were initiated at steps on the 6H-SiC film. The 3C-SiC layers contained a high density of stacking faults and microtwins caused primarily by the interfacial stresses generated by the mismatch in lattice parameters between AlN and β-SiC coupled with the very low stacking fault energy of SiC. This is the first report of the deposition of single crystal SiC/AlN/SiC thin film heterostructures on any substrate as well as the first report of the epitaxial growth of single crystal layers of binary materials with three different crystal structures.

*Present Address
Naval Research Laboratory, Code 6861
4555 Overlook Av., SW
Washington, DC 20375-5320

Interest in wide bandgap semiconductors for high-temperature and high-power electronic and short-wavelength optoelectronic applications has increased markedly within the past several years. Two materials which have generated much interest in this regard are SiC and AlN. The former occurs in over 250 polytypes which differ only in their stacking sequence along the closest-packed direction. The most common of these are the cubic 3C and the hexagonal 6H, where the number refers to the number of Si and C bilayers necessary to produce a unit cell in the direction of closest packing. The 3C polytype is also referred to as β-SiC. All other forms are known collectively as α-SiC. The bandgap (3.0 eV for 6H and 2.28 eV for 3C at room temperature) is indirect in all polytypes; thus, they cannot be used alone for laser applications.

Aluminum nitride has considerable potential for electronic and ultraviolet optoelectronic applications, particularly in severe environments, due to its large and direct bandgap (6.28 eV at 300°C), high melting point (in excess of 2000°C), high thermal conductivity (3.2 W/cm·K), and low dielectric constant (ε=9.0). It typically forms in the wurtzite (2H) structure; however, the cubic, zincblende (3C) phase has recently been produced via molecular beam epitaxy (MBE) techniques [1, 2]. Additional characteristics of the 2H polytype include a high resistivity and ease of oxygen incorporation during growth.

Epitaxial wurtzitic AlN has been deposited previously on SiC substrates [3–5]. Chu et al. [3] obtained monocrystalline AlN layers of up to 25 μm thickness on hexagonal SiC{0001} substrates by chemical vapor deposition (CVD) from 1200-1250°C. Sitar et al. [4] used an electron cyclotron resonance (ECR) plasma for decomposition of N_2 and Al and Ga effusion cells for growth of AlN/GaN superlattices by plasma-assisted, gas source MBE on α(6H)-SiC(0001) and Al_2O_3(0001) at 600°C. The thickness range of the AlN layers was 0.5–20nm. However, the properties of the individual AlN layers were not examined. Yoshida et al. [5] also employed gas–source MBE and the sources of solid Al and NH_3 to deposit single crystal AlN films on Si(111) and Al_2O_3(0001) and (01$\bar{1}$2) at 1000-1200°C. They noted their films were much smoother than CVD-grown material and rivaled bulk single crystal AlN. Conversely, Rutz and Cuomo [6] reported the deposition of monocrystalline SiC on a single crystal AlN film by pyrolysis of a SiC target at 1860°C. The AlN substrate was previously formed at 1000°C by reactive rf sputtering on a W(111) single crystal. However, thin-film growth of AlN/SiC/AlN or SiC/AlN/SiC heterostructures has not been reported to date.

Stable pseudomorphic heterostructures of AlN and SiC are feasible because of their similarity in crystal structure, lattice parameter and thermal expansion behavior. Theory regarding the electronic structure and bonding at SiC/AlN interfaces has been developed [7]. Critical layer thicknesses prior to misfit dislocation formation at pseudomorphic interfaces of cubic AlN and cubic SiC have been calculated [8]. Superlattices of these materials would have

a different band structure than either constituent element because the Brillouin zone is reduced in size in the direction normal to the interfaces, and certain superlattice states occur at different points in k space than the corresponding bulk material [9]. This may allow the resultant superlattice to have a direct band transition.

In the present research multiple layers of AlN and SiC were grown using a specially designed plasma-assisted gas-source molecular beam epitaxy (PAGSMBE) system. A schematic of this equipment is shown in Figure 1. This system is similar to that described previously for SiC MBE growth [10]. The precursors used for Si and C were Si_2H_6 and C_2H_4 (both 99.99% pure), respectively. Solid Al (99.999% pure) was evaporated from a standard effusion cell. Nitrogen was obtained by electron cyclotron resonance (ECR) plasma decomposition of N_2 (99.9995% pure). The system base and working pressures were 10^{-9} and 3×10^{-5} torr, respectively. Vicinal 6H-SiC(0001) wafers oriented 3-4° towards [11$\bar{2}$0] and containing a thermally oxidized(50nm) 0.8 μm epitaxial 6H-SiC layer deposited via CVD were obtained from Cree Research, Inc. and used as substrates in this research These substrates were chemically cleaned prior to growth in a 10% HF solution for five min. to remove the oxide, rinsed in DI H_2O for two min, immediately loaded into the growth system and heated for five min at the growth temperature of 1050°C. Additional growth conditions are listed in Table I.

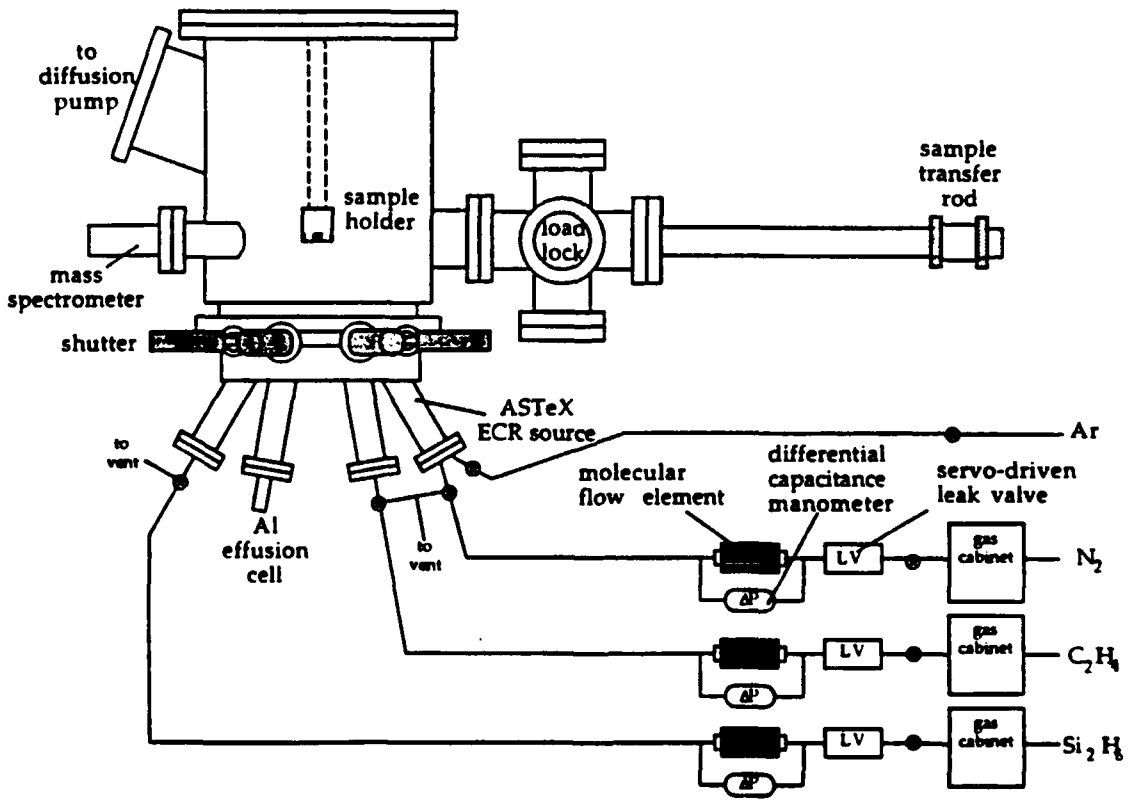

Figure 1. Schematic of gas-source molecular beam epitaxy system use to deposit the SiC and AlN films in this research.

Table I. Growth Conditions for the AlN and SiC Layers

AlN	
Growth temperature	1050°C
Nitrogen pressure	1.5×10^{-4} torr
Nitrogen flow rate	8 sccm
Microwave power	100 W
Growth rate	26 nm/hr
SiC	
Growth temperature	1050°C
Disilane flow rate	0.10 sccm
Ethylene flow rate	0.20 sccm
Growth rate	6.2 nm/hr

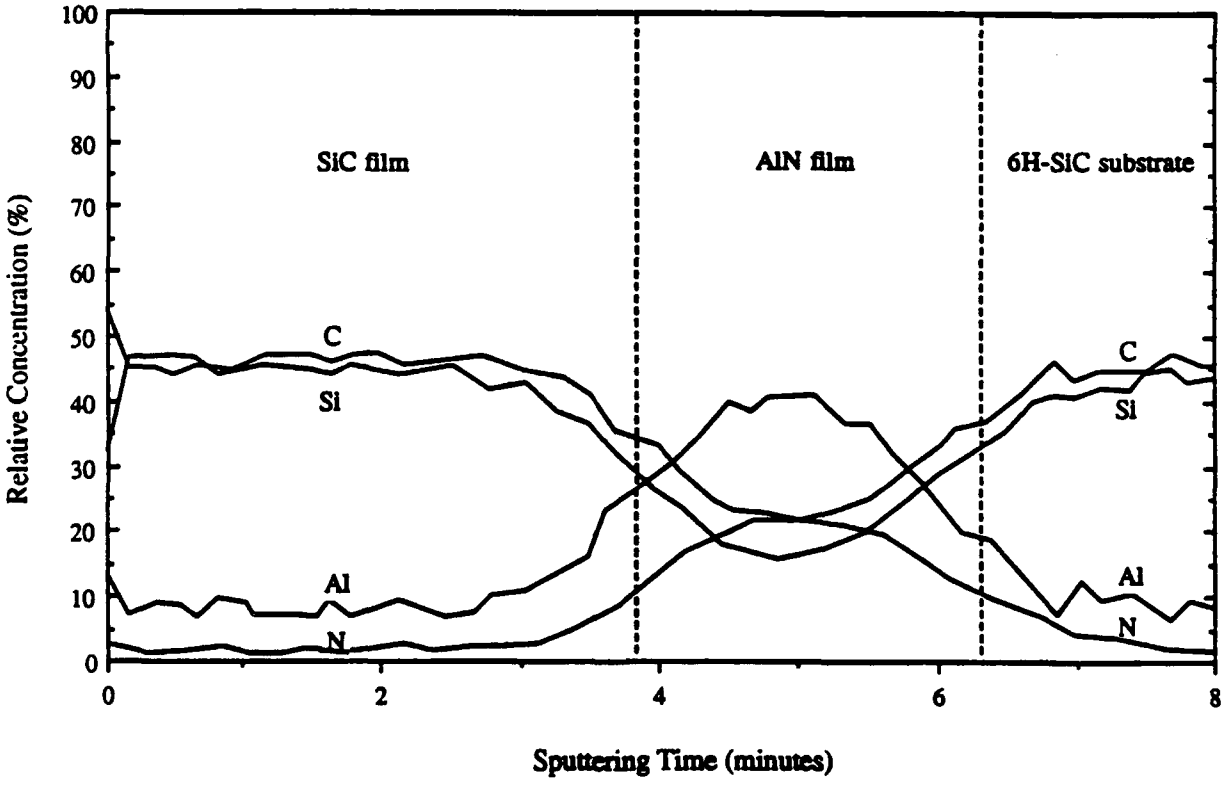

Figure 2. Auger depth profile of representative SiC/AlN/SiC multilayer heterostructure.

Reflection high-energy electron diffraction (RHEED) was used as an indicator of the quality and crystal structure of the resultant films. Figure 3 shows representative RHEED patterns for (a) the final growth surfaces of the films of AlN ([10$\bar{1}$0] azimuth) and (b) SiC ([110] aximuth). These patterns also show that both films were monocrystalline with the AlN having the 2H structure and the SiC the 3C modification, as indicated by the azimuthal assignments. The RHEED pattern of the top SiC layer also contains additional spots, as denoted by arrows in Figure 3(b). This pattern is fully indexed in Figure 4. It is probable that these extra spots arise from double positioning boundaries (DPBs). These incoherent twin boundaries occur when 3C-SiC (111) is grown on Si (111) [11] or on-axis 6H-SiC [12] because two different orientations, rotated 60° from each other, are present which have close-packed directions aligned in the interface. These different orientations differ in the cubic stacking sequence, as one orientation has an ...ABCABC... stacking sequence and the other has an ...ACBACB...stacking sequence. Extra reflections in the [110] RHEED pattern due to double positioning twins would either coincide with those of the film or be displaced by 1/3[111]. The extra spots present in the figure occur at 1/3 of the distance between adjacent spots in the [111] and [111] directions.

An equivalent interpretation of the RHEED pattern shown in Figure 3(b) is of two interpenetrating [110] RHEED patterns with a misorientation of 180°. This misorientation is caused by reflections from regions with both ...ABCABC... and ...ACBACB... sequences. The effect of each individual stacking sequence as well as the resultant RHEED pattern due to contributions of the two equivalent stacking sequences are shown in Figure 5.

Figure 6 shows a representative HRTEM image of the off-axis 6H-SiC (0001) substrate, the 2H-AlN layer, and the 3C-SiC layer. The interface between the SiC substrate and the AlN is abrupt with little change in contrast across it. The surface of the AlN film is smooth and uniform. The 2H-AlN and 6H-SiC films are in the same orientation in all directions, and the alignment of the atom columns is continuous across the interface. Thus, the AlN film is both epitaxial and pseudomorphic with respect to the substrate. Strain contrast, as evidenced by distortion in the lattice fringes, can be seen near steps in the SiC substrate surface, as denoted by arrows in Figure 6. Dislocations running parallel to the surface which arise from this strain can also be observed at or near each step.

The interface between the AlN and the top 3C-SiC layer is also abrupt, though some regions exist for which the transition between AlN and SiC becomes indiscernible. The lattice structural images show that the SiC layer is indeed cubic as well as epitaxial and pseudomorphic with the AlN. Several <111> stacking faults can be seen in the cubic SiC layer.

Previous PAGSMBE growth in this research of SiC on similar substrates at 1000–1050°C also resulted in 3C-SiC(111). This result, combined with those noted above, suggest that the cubic polytype forms preferentially at these temperatures under the conditions of low growth

(a)

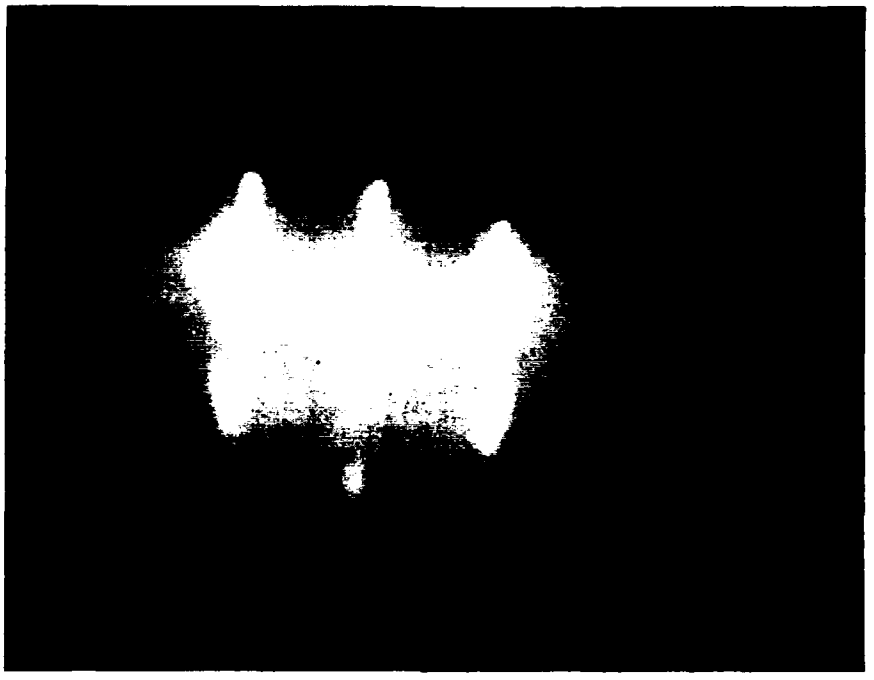

(b)

Figure 3. (a) RHEED pattern ([10$\bar{1}$0] azimuth) of the final surface of a monocrystalline 2H-AlN layer grown on α(6H)-SiC epitaxial layer.

(b) RHEED pattern ([110] azimuth) of the final surface of a monocrystalline 3C-SiC layer grown on 2H-AlN film. Arrows denote additional spots in the 3C-SiC layer (see Figures 4 and 5 for indexing).

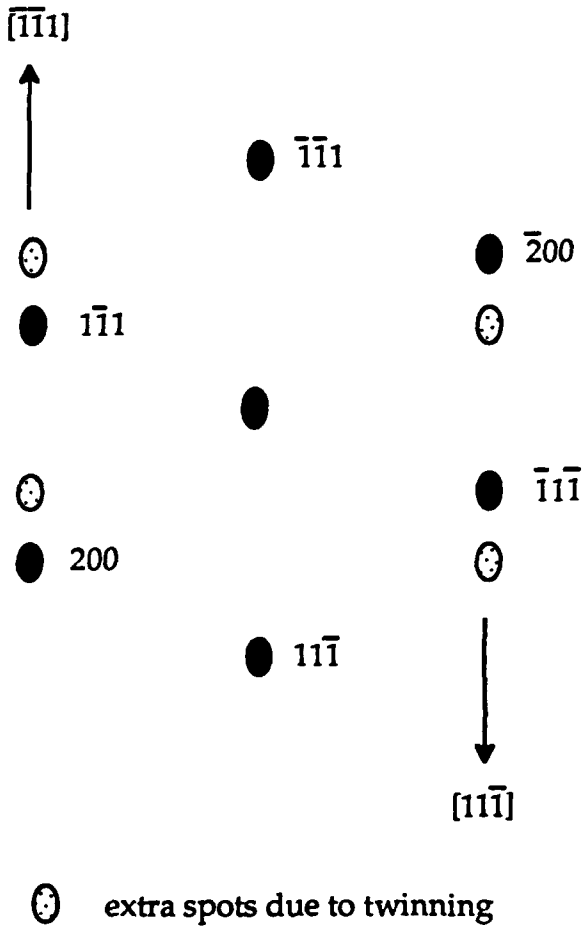

Figure 4. Indexed RHEED pattern ([110] azimuth) of 3C-SiC layer. Lighter spots are twin spots caused by double positioning boundaries.

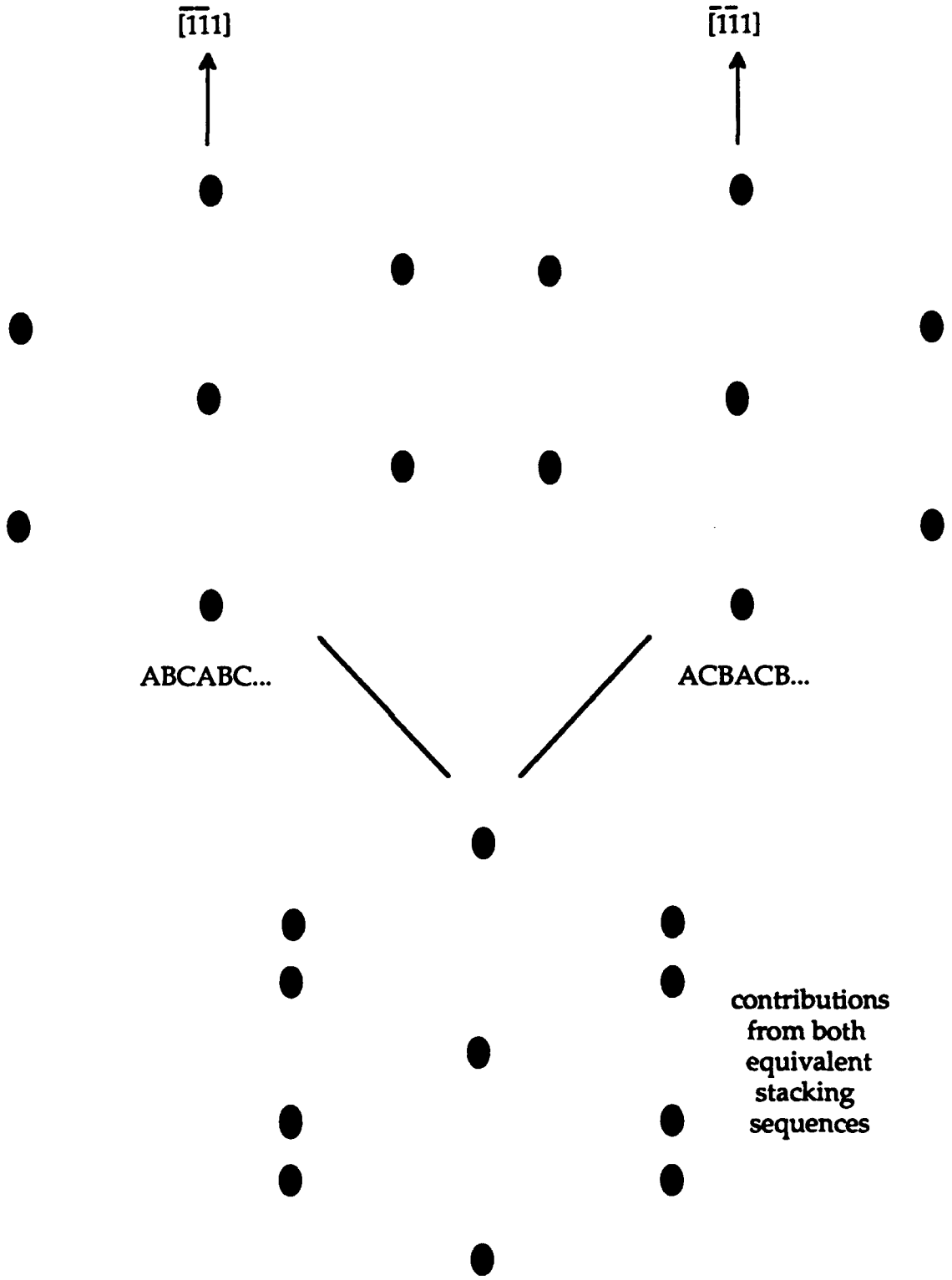

Figure 5. Effect of two equivalent stacking sequences of 3C-SiC (111) on [110] azimuth RHEED pattern.

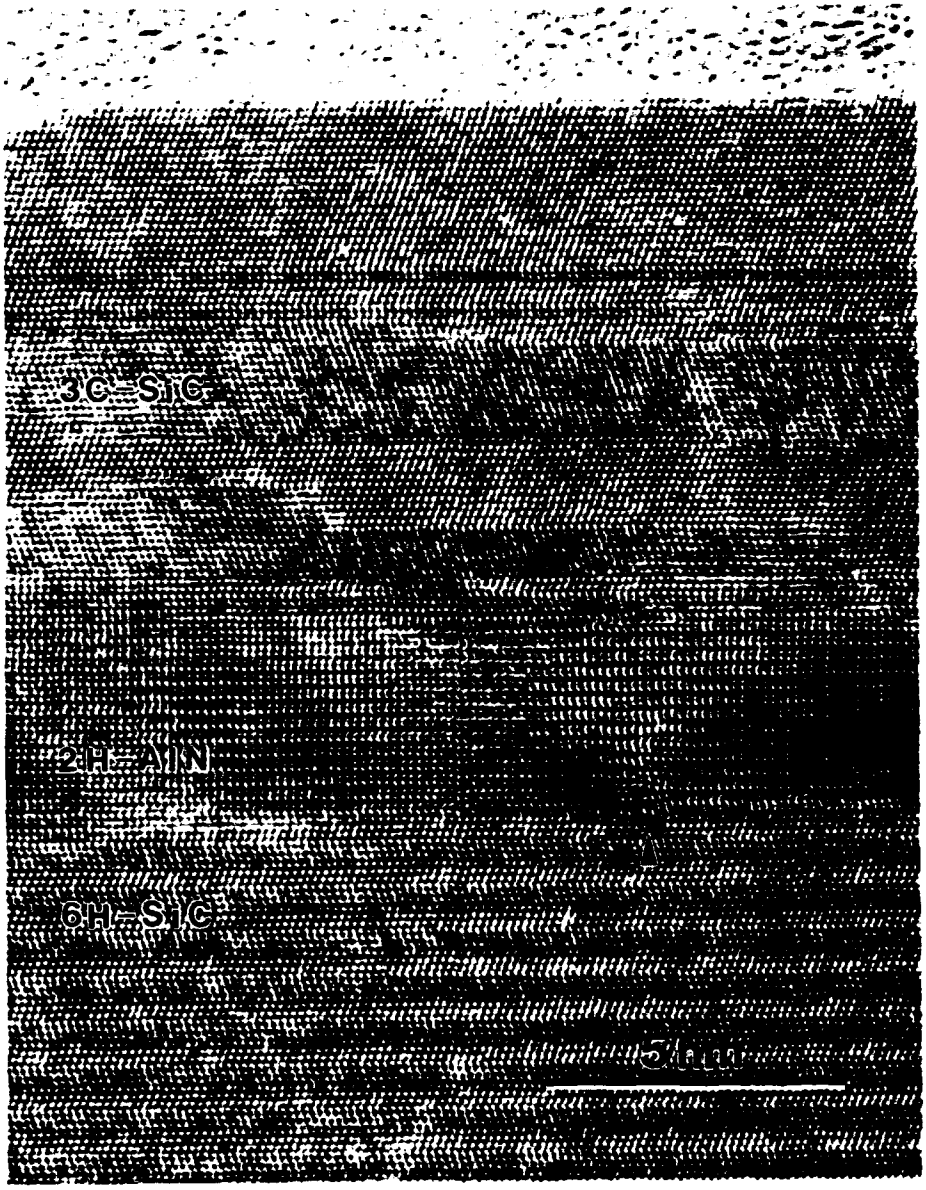

Figure 6. High-resolution transmission electron micrograph of epitaxial, pseudomorphic SiC/AlN/SiC multilayer heterostructure. Arrow shows a position of lattice distortion in the AlN associated with steps contained in and dislocations running parallel to the SiC surface.

rate and high supersaturation used in MBE. However, growth of SiC/AlN heterostructures at higher temperatures may result in hexagonal SiC layers, as atomic mobility on the AlN surface increases and the steps rather than the terraces become the templates for layer-by-layer growth. This trend towards the deposition of hexagonal SiC films at higher temperatures has been reported by several investigators[12-14]. It is also under study in the authors' laboratory and will be reported in the near future.

In summary, thin-film heterostructures composed of 3C-SiC, 2H-AlN and 6H-SiC have been achieved. The 3C-SiC and the AlN layers were grown at 1050°C using PAGSMBE. The diagnostic tools of RHEED and cross-sectional HRTEM showed both of these layers to exist in an epitaxial and pseudomorphic relationship with each other and with the 6H–SiC homoepitaxial layer deposited by CVD. To the authors' knowledge, this is the first report and direct observation of a single crystal SiC/AlN/SiC heterostructure on any substrate. It is also the first known report of the single-crystal growth of layers of binary materials in three different crystal structures (the 6H-SiC epilayer on the SiC wafer is counted in this case). These unique structures, composed of direct (AlN) and indirect (SiC) wide bandgap semiconductor materials undoubtedly possess important electronic, mechanical and thermal properties which are under investigation by the authors at this time.

The authors express their appreciation to the Office of Naval Research for support of this research under Grant #N00014-90-J-1427, to Cree Research, Inc. for the vicinal 6H-SiC wafers and epilayers and to Applied Science and Technology, Inc. for supplying the ECR plasma source. Appreciation is also expressed to S. Rogers for the Auger microprobe analysis.

REFERENCES

1. Z. Sitar, Ph. D. dissertation, North Carolina State University, 1990.
2. S. Strite and H. Morkoç, private communication.
3. T. L. Chu, D. W. Ing, and A. J. Norieka, Solid-State Electron. **10**, 1023 (1967).
4. Z. Sitar, M. J. Paisley, B. Yan, R. F. Davis, J. Ruan, and J. W. Choyke, Thin Solid Films **200**, 311 (1991).
5. S. Yoshida, S. Mizawa, Y. Fujii, S. Takada, H. Hayakawa, S. Gonda, and A. Itoh, J. Vac. Sci. Technol. **16**, 990 (1979).
6. R. F. Rutz and J. J. Cuomo, *Silicon Carbide-1973*, (U. of S.C., Columbia, 1974), p. 72.
7. W. R. L. Lambrecht and B. Segall, Phys. Rev. B **43**, 7070 (1991).
8. M. E. Sherwin and T. J. Drummond, J. Appl. Phys. **69**, 8423 (1991).
9. G. C. Osbourn, J. Vac. Sci. Technol. B **1**, 379 (1983).
10. L. B. Rowland, R. S. Kern, S. Tanaka, and R. F. Davis, in *Proceedings of the Fourth International Conference on Amorphous and Crystalline Silicon Carbide* (Springer-Verlag, Berlin), in press.
11. I. H. Khan and R. N. Summergrad, Appl. Phys. Lett. **11**, 12 (1967).
12. H. S. Kong, B. L. Jiang, J. T. Glass, G. A. Rozgonyi, and K. L. More, J. Appl. Phys. **63**, 2645 (1988).
13. R. B. Campbell and T. L. Chu, J. Electrochem. Soc. **113**, 825 (1966).
14. V. J. Jennings, A. Sommer, and H. C. Chang, J. Electrochem. Soc. **113**, 728 (1966).

VI. Determination of the Diffusivity of the Si, C, Al, and N at the Interface of the SiC-AlN Diffusion Couple

A. Introduction

SiC-based materials demonstrate promise as high temperature, optoelectronic, and acoustoelectronic wide bandgap semiconductors. Several attempts have been made to alloy SiC with other ceramic compounds in an attempt to engineer the mechanical and physical properties [1]. There have been numerous attempts to determine the existence of solid solutions of SiC-AlN. Cutler et al, under nitrogen atmosphere, obtained 2H SiC-AlN solid solutions from 2 to 100 mol % AlN through the carbothermal reduction at 1600°C of fine silica and alumina with a carbon source [2]. Jenkins et al. has reported growth of solid solutions over the entire pseudo binary phase diagram using metalorganic chemical vapor deposition (MOCVD) [3]. Kern has also reported the growth of solid solutions of $(AlN)_x(SiC)_{1-x}$ by plasma-assisted gas-source molecular beam epitaxy at temperatures of 1050°C [7].

There exists, however, a difference in opinion among investigators about the possibility of forming solid solutions or new phases in the SiC-AlN system at high temperatures [5]. Rafaniello *et al.* hot pressed SiC-AlN powder with 0.5 wt % C in alcohol and also obtained 2H solid solutions through the full range of compositions, but phase separation occurred upon annealing at 1700°C. This suggested the existence of a miscibility gap in the system in the low temperature range [8]. The difficulties encountered in the attempts to obtain homogeneous SiC-AlN solid solutions are known to be related to the low diffusion coefficients of Si and C in AlN and Al and N in SiC.

The diffusion coefficient of N in SiC has been determined to be 1×10^{-12} cm ^{2}-s^{-1} at 2550°C [6]. In hot pressed SiC-AlN samples and in SiC-AlN diffusion couples, approximate coupled diffusion coefficients of SiC and AlN were calculated to be 1×10^{-12} cm^2·s^{-1} [4]. The corresponding activation energy was roughly estimated to be as high as 900 kJ ·mol, and the pre-exponential term was 1×10^{-8} cm^2·s^{-1}, an unusually high value. Thus, it was suggested that lattice diffusion of coupled SiC and AlN pairs was responsible for these high values.

The purpose of this investigation is to determine the diffusion coefficient and the corresponding activation energy for the diffusion of the four elements Si, C, Al and N in the interface layer between the single crystal SiC and sintered AlN materials. Although the diffusion coefficient for N in SiC at high temperatures has been determined previously, never before have the diffusivities of these species been studied in single crystal SiC. The atomic behavior and phase formation at relatively low temperatures for thin film deposition have not been yet clarified. For this experiment, Auger spectroscopy and High Resolution Transmission Electron Microscopy have been employed to determine the nature and extent of the diffusion

profiles and the existence (or lack there of) of additional phases in the solid solution region and at the interfaces between the solution and the end-member phases.

B. Experimental Procedures

Sample Preparation. A SiC sample was prepared from a single crystal α-6H SiC [0001] wafer, cut off axis 3°–4° toward the [11$\bar{2}$0], manufactured by Cree Research, Inc. The SiC was cut into 4 mm squares with a diamond saw. Due to the extremely smooth surface provided by the epitaxial growth technique of Cree Research, Inc the SiC material was not polished. The AlN sample was prepared from sintered bulk material. It was cut into 4 mm squares, and polished using a L/P machine model 7 by Solid State Measurements, Inc. The lapping machine allows variable polishing angels. Diamond slurries were used for the polishing in steps of 30 micron, 6 micron, 1 micron, and 0.1 micron in order to get as close a match to the SiC face as possible.

Processing. The polished surface of SiC was placed on top of the AlN and loaded in the furnace prior to diffusion. The chamber is evacuated (2×10^{-6} torr) to prevent contamination during diffusion. N_2 gas (99.995%) is then introduced into the chamber at a rate of 130 sccm. The chamber is brought to atmospheric pressure and the N_2 environment is maintained throughout the diffusion. The N_2 is not meant to aid in the diffusion of N into SiC and does not to any appreciable amount. The sample was then heated to 1550 °C, a 20 pound normal load applied, and held for 3 hours. The load was applied to ensure that the SiC-AlN interface remained in intimate contact during chemical bonding. This coupled with the polishing of the AlN should eliminate surface impedance of the diffusion process. The load was then reduced to zero and the sample was taken to the diffusion temperature. The amount of time to take the sample to diffusion temperature is not entered into the time of diffusionat the longest time was only 10 minutes. Once the diffusion temperature was obtained it was held with no load for 200 hours. Ramp down to room temperature was done over a 1 1/2 hour time period to allow relaxation of the lattice and to avoid excess strain due to thermal and lattice mismatch of the SiC-AlN interface.

Characterization. *Auger spectroscopy.* The sample was lapped to an angle of 34 minutes which creates a simulated magnification of approximately 100 times the diffused layer. Samples were then polished using diamond slurries in steps of 6 micron, 1 micron, and 0.1 micron. Using the SiC wafer and AlN bulk material as standards for intensity ratio of 50 % Si to 50 % C, and 50 % Al to 50% N a concentration versus. distance profile was established of the diffused interface. In order to ensure more precise measurement of the diffused layer low currents were used to reduce the sampling size of the aperture. This coupled with the magnification of the interface allows for a greater certainty of results.

Transmission Electron Microscopy. The sample was cut into 3 micron wide and 500

micron thick dices which were mechanically thinned to about 100 micron and dimpled at the SiC-AlN interface to a final thickness of 20 micron. Further thinning of the samples with an ion miller achieves a electron transparent area. An acceleration voltage of 6 kV for initial milling was used and decreased to 4 kV for finish milling. The milling angles of 15°,12°, and 6° were used during the milling step-wise. TEM observations were then carried out using Akashi EM-002B Ultra-High Resolution TEM at 200 kV.

C. Results

Figure 1 shows the cross sectional TEM image of SiC-AlN diffused at 1600 °C for 200 hrs. Inserted pictures indicate the selected area diffraction patterns (SAD) taken at several regions referring to the numbers shown in the image. The following are brief explanation of each pattern.

1. SiC region, showing 6H(hexagonal)-SiC with [11$\bar{2}$0] zone axis.
2. SiC/AlN interface region, showing the mixture of patterns 1 and 3.
3. AlN region, showing different orientations of the grains.
4. SiC/AlN interface region of a different grain in AlN, showing the mixture of patterns 1 and 5.
5. AlN region, showing a long range ordered polytype.
6. AlN region, showing 2H crystalline structure.

Note the new phase at the interface of the diffused SiC-AlN which has a different crystal structure. It has a longer range order crystal structure than 6H structure. Chemical analysis such as EDS and EELS are desired to identify the phase and its composition.

Figure 2 shows the High Resolution TEM (HRTEM) image of the diffusion area. The image was taken with multi-beam condition and the zone axis was [11$\bar{2}$0]. To the left between the α-6H SiC and the 2H-AlN is an example of long range ordering in the diffused region.

Concentration versus distance profiles for 1500°C and 1600°C have been completed. Figure 3 a-d show line scan profiles for each element at 1500°C for 200 hrs. Notice the sharp drop off of the intensity. This indicates that there is little or no diffusion. The roughness of the line scan is due to the low signal to noise ratio and roughness of the surface. Signal to noise ratio is large to lower the beam spot size. This allows an increase in the accuracy of measuring the diffused layer. However careful analysis of the data concludes that even with a magnification of the interface and very small beam size, approximately 1.2 micron, reliable results are hard to achieve without substantial experimental error. In this case a sampling size of 1.2 microns and supposed diffusion distance of 2.5 microns. Therefore no conclusion can be obtained without further analysis. Lower beam currents will reduce the beam sampling size, however, limiting that is the charging effects of the highly insulating materials.

Figure 1. Cross-sectional TEM image of SiC-AlN at 1600°C for 200 hrs. and SAD patterns in several regions.

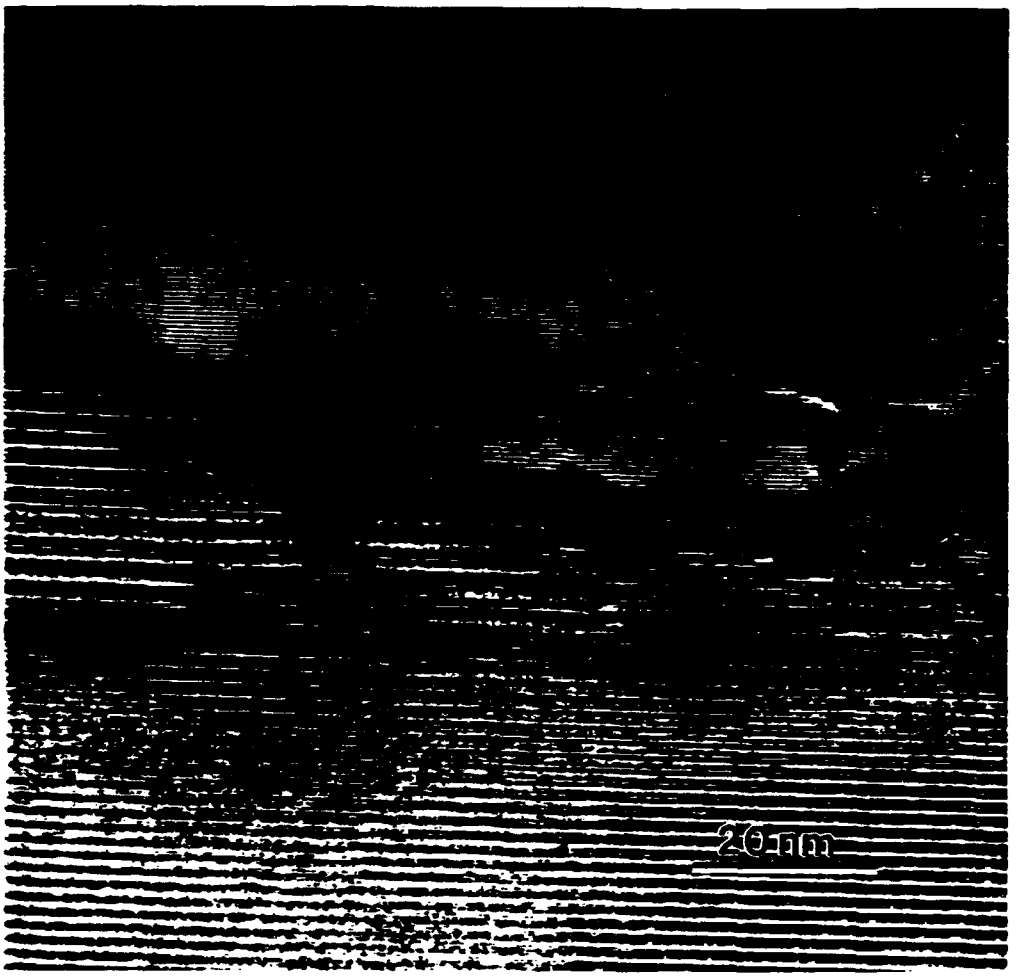

Figure 2. Cross-sectional HRTEM image of interface region of SiC-AlN at 1600°C for 200 hours.

E. Discussion

Further studies of the SiC-AlN diffusion coupled system are necessary for the determination of the diffusion coefficients with any certainty. Solid solutions at the interface have been observed and are being quantified. We have determine that at temperatures of less than 1500°C and for times of 200 hrs that significant diffusion is not observed. This is good news for the stable growth of solid solutions of SiC-AlN at relatively high temperatures for such growth process as MBE and MOCVD. There are several limiting factors in the diffusion of SiC-AlN. Many of which can not be controlled in this experiment. Oxidation of the SiC and AlN surfaces is one example which hinders the diffusion. Another problem more so than the oxidation is the roughness of the surface which definitely slows the diffusion mechanism. One possible approach to the elimination of these errors is to grow AlN on SiC and then study the diffusion process. Higher temperature diffusions and better accuracy in measurement of

the diffused region will enable the determination of the diffusion coefficients of the four species.

F. Future Research Plans/Goals

1. Determination of temperature dependence of any new phase formation near the interface of the SiC/AlN system. This would be determined by the use of different times at the same temperature.
2. Determination of time dependence of diffusion coefficient for the four elements moving as individual diffusion elements or moving as couples.
3. Determination of concentration versus distance profiles using EDS.
4. Use MBE grown AlN on SiC to eliminate contamination of the interface, and to obtain a epitaxially smooth surfaces which also eliminated the limiting of surface roughness on the diffusion process.

G. References

1. A. Zangvil and R. Ruh, J. Mat. Sci. and Engr. 71 159 (1985).
2. I. B. Cutler, P. D. Miller, W. Rafaniello, H. K. Park, D. P. Thompson, and K. H. Jack, Nature (London), 275 [5679]434-35 (1978).
3. I. Jenkins, K. G. Irvine, M. G. Spencer, V. Dmitriev, and N. Chen, in press.
4. W. F. Knippenberg et al., U.S. Patent No. 3,634,149 1972.
5. N. D. Sorokin, Yu. M. Tairov, and V. F. Tsvetkov, Abstracts of Reports at the Third All-Union Symposium on Scanning Electron Microscopy and Analytic Methods for Studying Solids, Zvenigoro, Nauka, Moscow, 227 (1981).
6. Y. A. Vodakov, and E.N. Mokhov, Silicon Carbide, 508-19 (1973).
7. R. S. Kern, L. B. Rowland, S. Tanaka, and R. F. Davis, to be published.
8. W. Rafaniello, K. Cho, A.V. Virkar, J. Mater. Sci. **16**, 3479 (1981).

LINESCAN PROFILE OF SAMPLE #8; Si

File : 8D.SLP

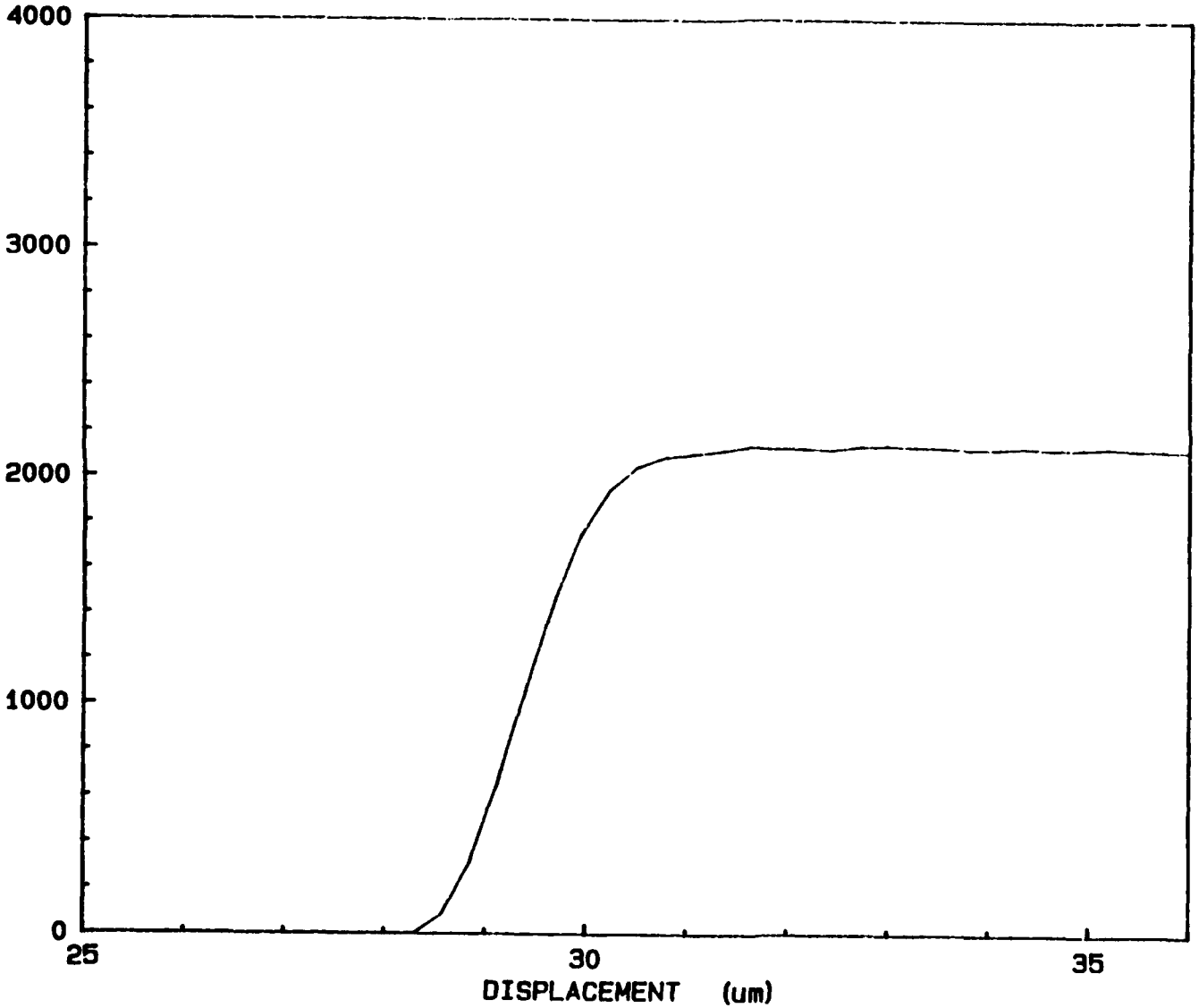

Date :	17-NOV-92	
Time :	16: 16: 04	
Acc.V	3.00	kV
Ip	$1.58*10^{-8}$	A
Vac.P	$4.8 *10^{-7}$	Pa
Vcem	2.5	kV
Vmod	8	eVp-p
Sen	1.00	mV
TC	1000	ms
#Pixels	200	
T.Time	6.87	min
Peak	78	eV
Bkg	91	eV
P.Calcu	P-B	
Dwell	1024	ms
Mag	2500	

Operator : D. RICKS

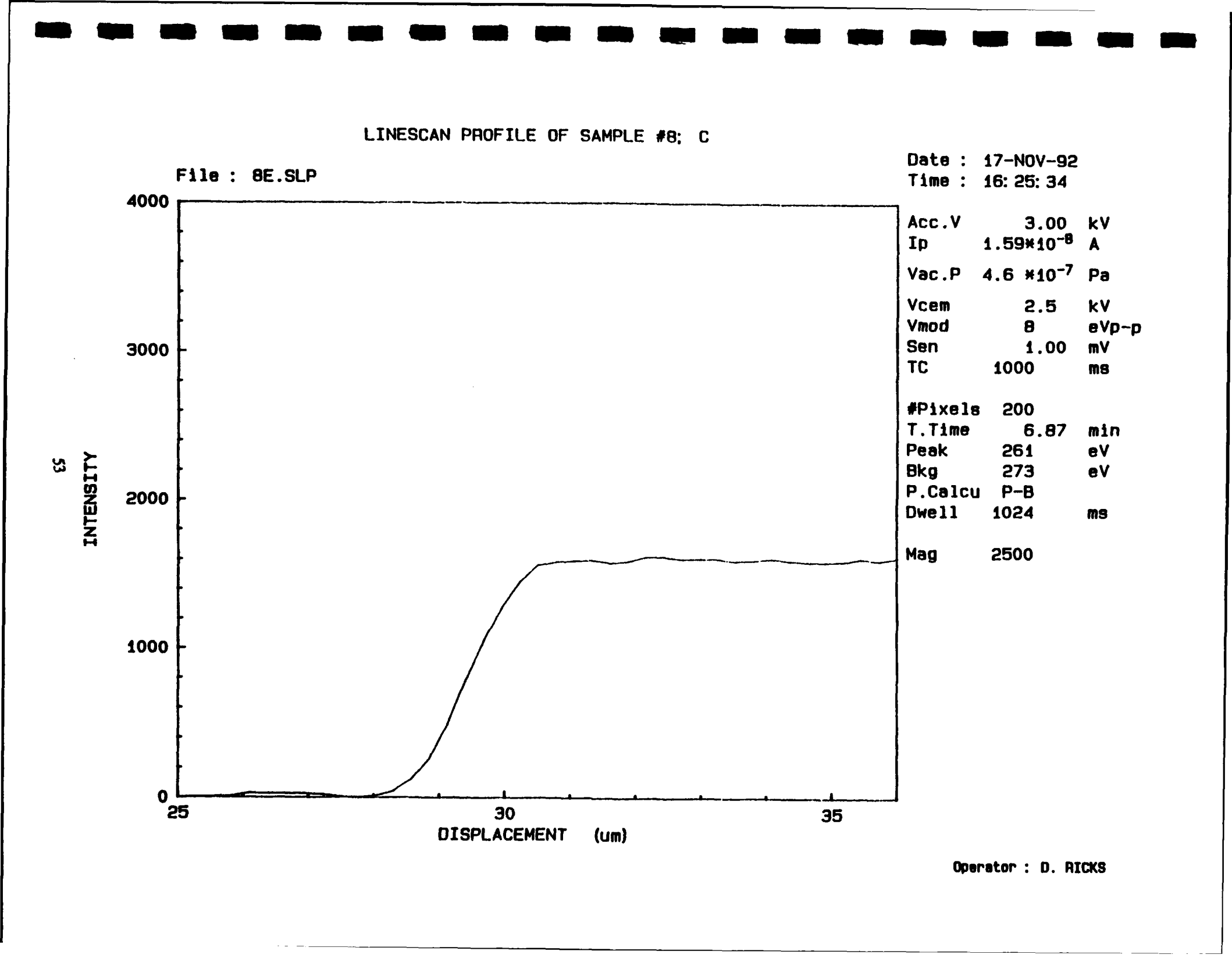
LINESCAN PROFILE OF SAMPLE #8; C
File : 8E.SLP
Date : 17-NOV-92
Time : 16:25:34
Acc.V 3.00 kV
Ip 1.59*10^-8 A
Vac.P 4.6 *10^-7 Pa
Vcem 2.5 kV
Vmod 8 eVp-p
Sen 1.00 mV
TC 1000 ms
#Pixels 200
T.Time 6.87 min
Peak 261 eV
Bkg 273 eV
P.Calcu P-B
Dwell 1024 ms
Mag 2500
4000
3000
2000
1000
0
INTENSITY
25
30
35
DISPLACEMENT (um)
Operator : D. RICKS

LINESCAN PROFILE OF SAMPLE #8; Al

File : 8B.SLP

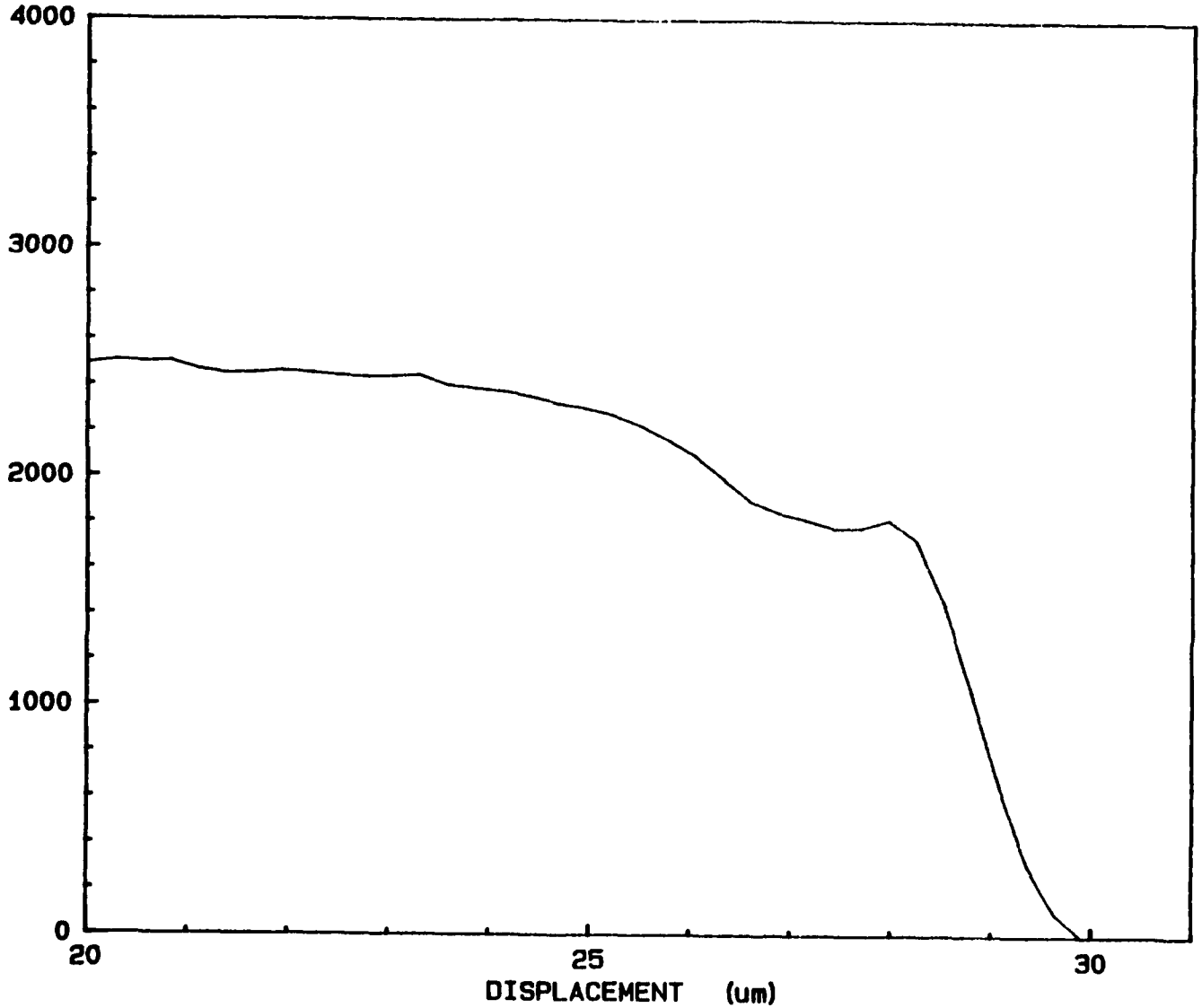

Date :	17-NOV-92	
Time :	15:56:51	
Acc.V	3.00	kV
Ip	$1.57*10^{-8}$	A
Vac.P	$5.4*10^{-7}$	Pa
Vcem	2.5	kV
Vmod	8	eVp-p
Sen	1.00	mV
TC	1000	ms
#Pixels	200	
T.Time	6.87	min
Peak	48	eV
Bkg	57	eV
P.Calcu	P-B	
Dwell	1024	ms
Mag	2500	

Operator : D. RICKS

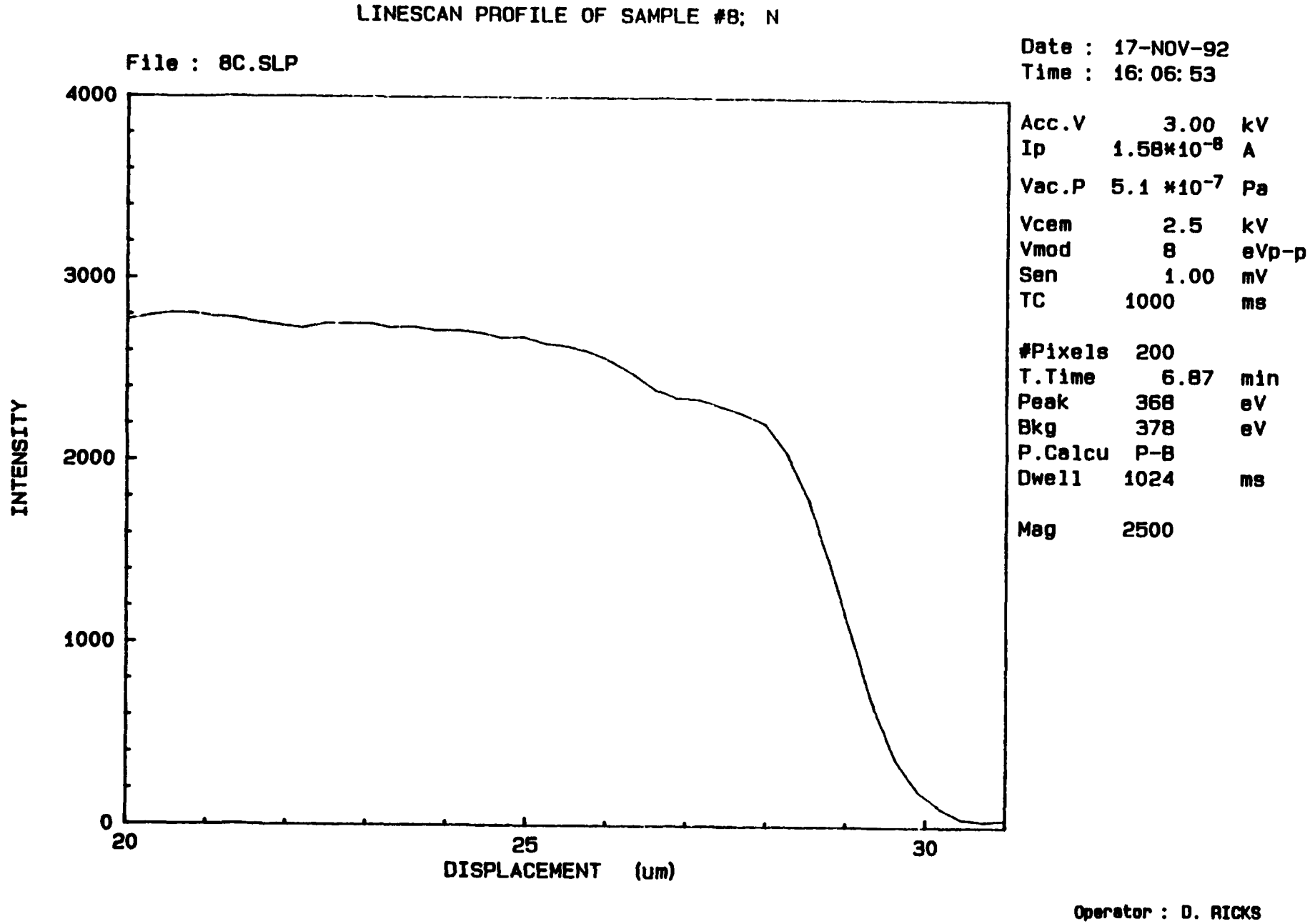
LINESCAN PROFILE OF SAMPLE #8; N
File : 8C.SLP
Date : 17-NOV-92
Time : 16:06:53
Acc.V 3.00 kV
Ip 1.58*10-8 A
Vac.P 5.1 *10-7 Pa
Vcem 2.5 kV
Vmod 8 eVp-p
Sen 1.00 mV
TC 1000 ms
#Pixels 200
T.Time 6.87 min
Peak 368 eV
Bkg 378 eV
P.Calcu P-B
Dwell 1024 ms
Mag 2500
4000
3000
2000
1000
0
INTENSITY
20
25
30
DISPLACEMENT (um)
Operator : D. RICKS

VII. Solid Solutions of AlN and SiC Grown by Plasma-Assisted, Gas-Source Molecular Beam Epitaxy

A Communication Submitted for Consideration for Publication
to
The Journal of Materials Research

by

R. S. Kern, L. B. Rowland*, S. Tanaka, and R. F. Davis
North Carolina State University
Department of Materials Science and Engineering
Box 7907
Raleigh, NC 27695-7907

November 1992

ABSTRACT

Solid solutions of aluminum nitride (AlN) and silicon carbide (SiC), the only intermediate phases in their respective binary systems, have been grown at 1050°C on α(6H)-SiC (0001) substrates cut 3-4° off-axis toward [11$\bar{2}$0] using plasma-assisted, gas-source molecular beam epitaxy. A film having the approximate composition of $(AlN)_{0.3}(SiC)_{0.7}$, as determined by Auger spectrometry, was selected for additional study and is the focus of this note. High resolution transmission electron microscopy (HRTEM) revealed that the film was monocrystalline with the wurtzite (2H) crystal structure.

* Present address: Naval Research Laboratory, Code 6861, 4555 Overlook Ave. SW, Washington, D. C. 20375-5000.

Silicon carbide is a wide bandgap material that exhibits polytypism, a one-dimensional polymorphism arising from the various possible stacking sequences of, e. g., the silicon and carbon layers along the directions of closest packing. The single cubic polytype, β-SiC, crystallizes in the zincblende structure, has a room temperature bandgap of 2.3 eV, and is commonly referred to as 3C-SiC. The three (3) refers to the number of Si and C bilayers necessary to produce a unit cell and the C indicates its cubic symmetry. There are approximately 250 other rhombohedral and hexagonal polytypes[1] that are classed under the heading of α-SiC. The most common of these latter polytypes is 6H-SiC with a room temperature bandgap of ≈ 3.0 eV.

Aluminum nitride normally occurs in the wurtzite (2H) structure; however, the cubic, zincblende phase has been produced[2,3]. The 2H polytype possesses a direct bandgap[4] and a thermal conductivity[5] of 6.28 eV and 3.2 W/cm°K, respectively. As such, this material is of particular interest for high power and optoelectronic devices, the latter of which would emit and absorb ultraviolet radiation.

Solid solutions of AlN and SiC have been achieved by two primary routes: reactive sintering of mixtures of powders of a variety of sources and thin film deposition from the vapor phase. Matignon[6] first reported the synthesis of a $(AlN)_x(SiC)_{1-x}$ material in 1924 formed by heating Al_2O_3, SiO_2, and coke in the presence of flowing N_2 at an unspecified temperature. Related hot pressing and annealing research coupled with X-ray diffraction and optical and electron microscopy by Rafaniello et al.[7,8] reportedly resulted in single phase, 2H material at all compositions hot pressed at 2300°C but only within the ranges of 0-15 and 75-100 wt% AlN for samples prepared at 2100°C and below. This latter result indicated a miscibility gap, the existence of which was subsequently confirmed by Zangvil and Ruh[9-12], Kuo and Virkar[13], and Czeka et al.[14] using a variety of heat treatment schedules. The tentative phase diagram proposed by Zangvil and Ruh[11] shows a flat miscibilty gap at 1900°C between ≈ 8 and 95 wt% AlN. Above this temperature a 2H solid solution was reported from ≈ 20-100 wt% AlN. From 0-20 wt% AlN, solutions and two phase mixtures of 6H, 4H, and 2H were observed.

Thin film solid solutions have been produced in the Soviet Union[15] via sublimation of a sintered SiC/AlN compact at ≥ 2100°C and in the United States[16] using low pressure (10-76 Torr) metalorganic chemical vapor deposition (MOCVD) and the sources of SiH_4, C_3H_8, NH_3, and $Al(CH_3)_3$ carried in H_2. The former research also showed that at T ≥ 2100°C, solid solutions having the 2H structure could be produced at compositions of AlN ≥ 20 wt%. By contrast, Jenkins et al.[16], have reported the MOCVD growth of solid solutions over the entire pseudobinary phase diagram. The composition of these films, grown from 1200-1250°C, was strongly dependent on the system pressure, which varied from 10-76 Torr. Electron channeling patterns on selected films indicated that the films were monocrystalline.

Films having cubic symmetry were obtained on Si (100) substrates; hexagonal films were deposited on α(6H)-SiC (0001) wafers.

In the present research, a specially designed and previously described[17] plasma-assisted, gas source molecular beam epitaxy system was employed to deposit $(AlN)_x(SiC)_{1-x}$ thin film solid solutions on α(6H)-SiC (0001) substrates obtained from Cree Research, Inc. and oriented 3.5 ± 0.5° off (0001) toward [11$\bar{2}$0]. The substrates were chemically cleaned before growth in a 10% HF solution for 5 minutes, followed by a DI water rinse for 2 minutes, and loaded immediately into the growth chamber. Sources of Si and C were disilane, Si_2H_6, and ethylene, C_2H_4, respectively. Aluminum (99.999% purity) was evaporated from a standard MBE effusion cell. A compact electron cyclotron resonance (ECR) plasma source supplied by ASTeX, Inc., was used to decompose N_2 (99.9995% purity) diluted with ultra-high purity Ar to obtain sufficient electron-atom collisions to sustain a plasma. The growth conditions for the composition chosen for additional study are listed in Table I.

Table I. Growth Conditions for $(AlN)_{0.3}(SiC)_{0.7}$ Thin Films

Chamber Base Pressure	10^{-9} Torr.
Deposition Pressure	10^{-4} Torr.
Deposition Temperature	1050°C
Flow Rate (Si_2H_6)	0.75 sccm
Flow Rate (C_2H_4)	3.75 sccm
Ar:N_2 Ratio	20:1
ECR Power	100 W
Aluminum Cell Temperature	1260°C
Deposition Time	2 hours

Reflection high-energy electron diffraction (RHEED) was used to determine the crystalline quality of the surface of the resulting films. The chemical composition as a function of film thickness was determined using a scanning Auger microprobe with Zalar rotation capability[18]. High-resolution transmission electron microscopy (HRTEM) was employed to observe the microstructure of the film as well as the film/substrate interfacial region.

Figure 1 shows an Auger depth profile of a selected solid solution film. Use of pure AlN and SiC standards and appropriate Auger sensitivity factors for each element showed the composition to be approximately $(AlN)_{0.3}(SiC)_{0.7}$.

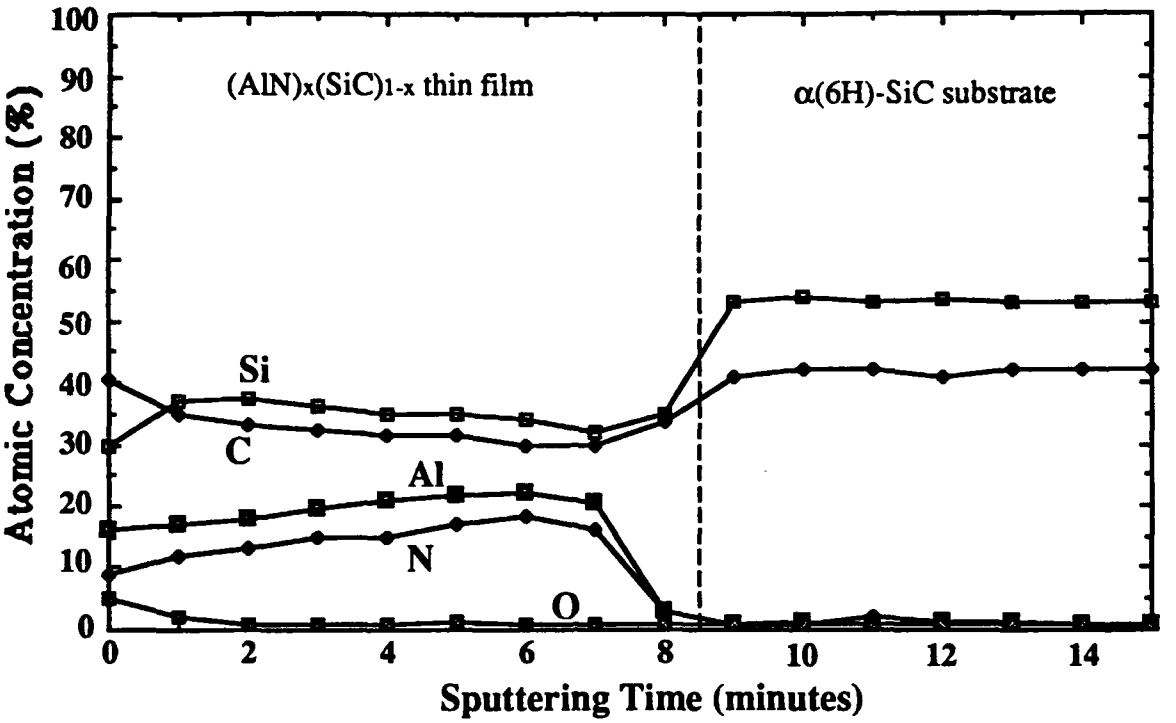

Figure 1. Auger depth profile of a $(AlN)_x(SiC)_{1-x}$ thin film ($x \approx 0.3$) showing relative atomic concentration versus sputtering time for each of the components.

The RHEED pattern indicated that the film was monocrystalline. This was confirmed using HRTEM. An image of the film and substrate used to obtain the Auger profiles is shown in Figure 2. The ...ABABAB... stacking sequence in the solid solution region shows that it possesses the wurtzite (2H) crystal structure. The fast Fourier transform pattern shown in the inset is that of the $[11\bar{2}0]$ azimuth for this structure. The random distribution of contrast is due to the elastic strain and slight buckling in the film. No second phase was observed within the film.

The resulting $(AlN)_x(SiC)_{1-x}$ thin films are, to the authors' knowledge, the first MBE grown alloys containing these components. The temperature of growth is also the lowest reported for these materials. This method of bandgap engineering is particularly interesting from the standpoint of the materials involved. AlN is a direct transition material, while SiC is an indirect one. Solid solutions of the wurtzite crystal structure (2H) should have E_g from 3.33 eV to 6.28 eV. Experimental optical characterization by Nurmagomedov et al.[14] has indicated that the bandgap is direct from 70-100 wt% AlN. The bandgap of cubic AlN has been theoretically estimated to be ≈ 5.11 eV at absolute zero and is believed to be indirect[15]. Therefore, cubic solid solutions should have E_g from 2.28 eV to roughly 5.11 eV and would probably be indirect at all compositions.

Epitaxial $(AlN)_x(SiC)_{1-x}$ alloys have been grown on α(6H)-SiC (0001) substrates by plasma-assisted gas-source molecular beam epitaxy at 1050°C. The $(AlN)_{0.3}(SiC)_{0.7}$ composition was selected for additional study. Analyses by RHEED and HRTEM showed this film to be monocrystalline and to exhibit the wurtzite (2H) crystal structure. This is the first known report of a single crystal $(AlN)_x(SiC)_{1-x}$ alloy grown by MBE.

The authors acknowledge The Office of Naval Research for the sponsorship of this research under Contract Number N00014-88-K-0341, Cree Research, Inc. for the vicinal 6H-SiC substrates, Applied Science and Technology, Inc. for the ECR plasma source, R. L. Moore at Evans East for the AES analysis, and J. Bentley of Oak Ridge National Laboratories for helpful discussions. This research was also partially sponsored by the Division of Materials Sciences, United States Department of Energy, under contract DE-AC05-840R21400 with Martin Marietta Energy Systems, Inc., and through the SHaRE Program under contract DE-AC05-760R00033 with Oak Ridge Associated Universities.

REFERENCES

1. G. R. Fisher and P. Barnes, Philos. Mag. B **61**, 217 (1990).
2. Z. Sitar, M. J. Paisley, and R. F. Davis, Annual Progress Report, ONR Contract N00014-86-K-0686, June 1, 1989.
3. S. Strite and H. Makoç, private communication.
4. G. A. Slack, J. Phys. Chem. Solids **34**, 321 (1973).
5. W. M. Yim, E. J. Stofko, P. J. Zanzucci, J. I. Pankove, M. Ettenberg, and S. L. Gilbert, J. Appl. Phys. **44**, 292 (1973).
6. C. Matignon, Compt. Rend. hu. L'Acad. Sci. **178**, 1615 (1924).
7. W. Rafaniello, K. Cho, and A. V. Vikar, J. Mat. Sc. **16**, 3479 (1981).
8. W. Rafaniello, M. R. Plinchta, and A. V. Vikar, J. Am. Ceram. Soc. **66**, 272 (1983).
9. R. Ruh and A. Zangvil, J. Am. Ceram. Soc. **65**, 260 (1982).
10. A. Zangvil and R. Ruh, Mat. Sc. Eng. **71**, 159 (1985).
11. A. Zangvil and R. Ruh, J. Am. Ceram. Soc. **71**, 884 (1988).
12. A. Zangvil and R. Ruh in *Silicon Carbide '87*, American Ceramic Society, Westerville, OH, 1989, pp. 63-82.
13. S. Kuo and A. V. Vikar, J. Am. Ceram. Soc. **73**, 2460 (1990).
14. C. L. Czkaj, M. L. J. Hackney, W. J. Hurley, Jr., L. V. Interrante, G. A. Sigel, P. J. Schields, and G. A. Slack, J. Am. Ceram. Soc. **73**, 352 (1990).
15. Sh. A. Nurmagomedov, A. N. Pitkin, V. N. Razbegaev, G. K. Safaraliev, Yu. M. Tairov, and V. F. Tsvetkov, Sov. Phys. Semicond. **23**, 100 (1989).
16. I. Jenkins, K. G. Irvine, M. G. Spencer, V. Dmitriev, and N. Chen, in press.
17. L. B. Rowland, S. Tanaka, R. S. Kern, and R. F. Davis, in *Proceedings of the Fourth International Conference on Amorphous and Crystalline Silicon Carbide* (Springer-Verlag, Berlin, 1992), in press.
18. A. Zalar, Thin Solid Films **124**, 223 (1985).

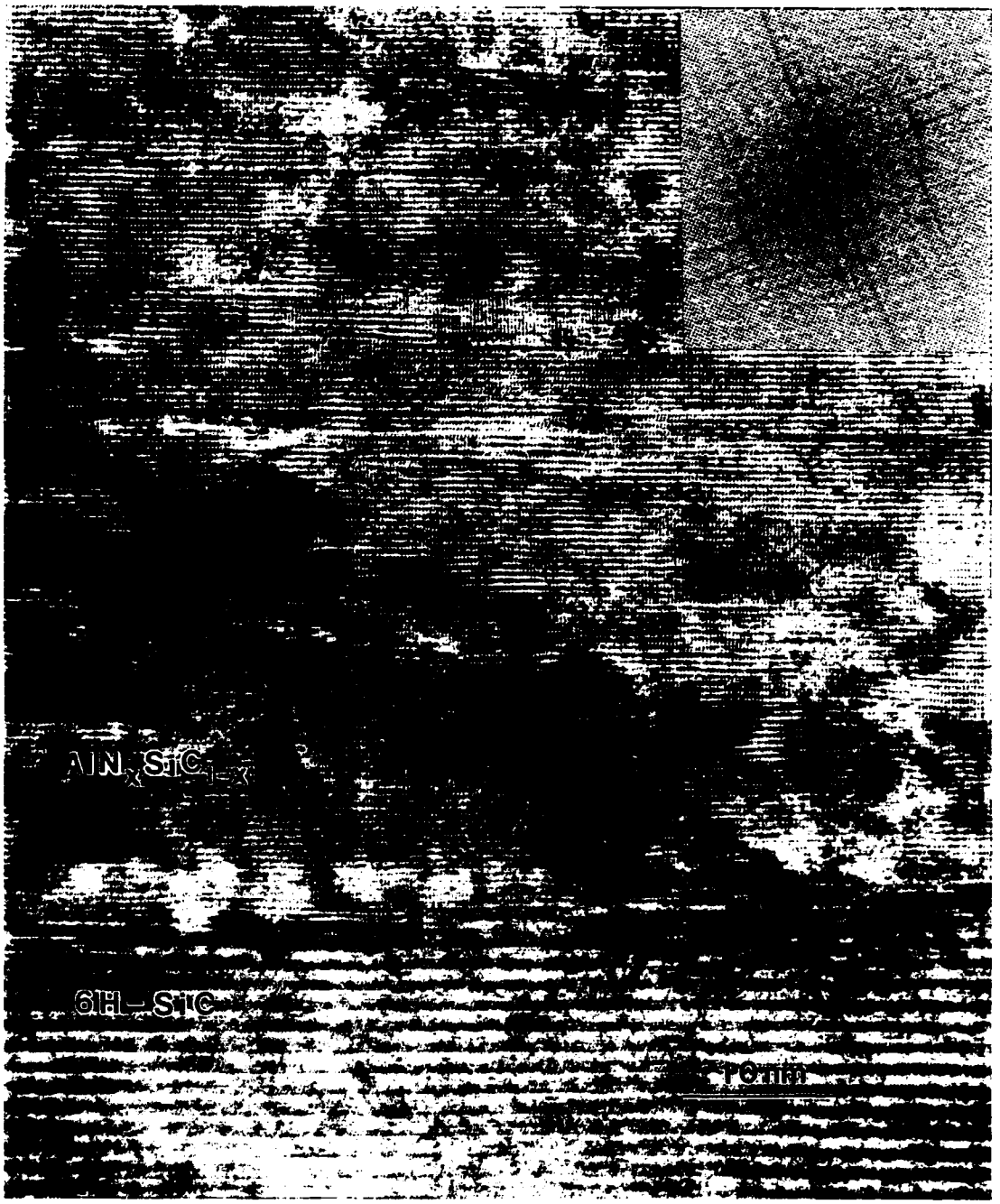

Figure 2. High-resolution transmission electron micrograph of the 2H $(AlN)_x(SiC)_{1-x}$ thin film grown on an α(6H)-SiC (0001) substrate and used to obtain the Auger depth profile in Figure 1.

VIII. Final Technical Report Distribution List

	Number of Copies
Dr. Yoon Soo Park Office of Naval Research Applied Research Division Code 1212 800 N. Quincy Street Arlington, VA 22217-5000	2
Administrative Contracting Officer Office of Naval Research Resident Representative The Ohio State Univ. Research Ctr. 1960 Kenny Road Columbus, OH 43210-1063	2
Director Naval Research Laboratory ATTN: Code 2627 Washington, DC 20375	7
Defense Technical Information Center Bldg. 5, Cameron Station Alexandria, VA 22314	14